Immunological imprinting shapes the specificity of human antibody responses against SARS-CoV-2 variants

Timothy S. Johnston[1,2,3,6], Shuk Hang Li[1,6], Mark M. Painter[2,4,6], Reilly K. Atkinson[1], Naomi R. Douek[2,4], David B. Reeg[2,5], Daniel C. Douek[3], E. John Wherry[2,4*], Scott E. Hensley[1,2*]

[1]Department of Microbiology, University of Pennsylvania Perelman School of Medicine; Philadelphia, PA
[2]Institute for Immunology and Immune Health, University of Pennsylvania Perelman School of Medicine; Philadelphia, PA
[3]Vaccine Research Center, NIAID, NIH; Bethesda, MD
[4]Department of Systems Pharmacology and Translational Therapeutics, University of Pennsylvania Perelman School of Medicine; Philadelphia, PA
[5]Department of Medicine II (Gastroenterology, Hepatology, Endocrinology and Infectious Diseases), Freiburg University Medical Center, Faculty of Medicine, University of Freiburg, 79106 Freiburg, Germany.

[6]These authors contributed equally

*Correspondence: wherry@pennmedicine.upenn.edu and hensley@pennmedicine.upenn.edu

Summary

The spike glycoprotein of severe acute respiratory syndrome coronavirus-2 (SARS-CoV-2) continues to accumulate substitutions, leading to breakthrough infections of vaccinated individuals and prompting the development of updated booster vaccines. Here, we determined the specificity and functionality of antibody and B cell responses following exposure to BA.5 and XBB variants in individuals who received ancestral SARS-CoV-2 mRNA vaccines. BA.5 exposures elicited antibody responses that primarily targeted epitopes conserved between the BA.5 and ancestral spike, with poor reactivity to the XBB.1.5 variant. XBB exposures also elicited antibody responses that targeted epitopes conserved between the XBB.1.5 and ancestral spike. However, unlike BA.5, a single XBB exposure elicited low levels of XBB.1.5-specific antibodies and B cells in some individuals. Pre-existing cross-reactive B cells and antibodies were correlated with stronger overall responses to XBB but weaker XBB-specific responses, suggesting that baseline immunity influences the activation of variant-specific SARS-CoV-2 responses.

Keywords

SARS-CoV-2, mRNA vaccines, Omicron BA.5, XBB.1.5, antibodies, B cells, original antigenic sin, immune imprinting, immune evasion, viral evolution

Highlights

- Variant breakthrough infections boost ancestral cross-reactive antibodies and B cells
- First and second BA.5 exposures fail to elicit variant-specific antibodies and B cells
- XBB infections and monovalent vaccinations elicit XBB.1.5-specific responses in some individuals
- XBB.1.5-specific responses correlate with low levels of pre-existing humoral immunity

Introduction

SARS-CoV-2 first emerged in 2019, prompting the rapid development of mRNA-LNP vaccines that elicit potent neutralizing antibodies targeting the viral spike glycoprotein (Corbett et al., Hseih et al., Jackson et al., 2020). The virus has since acquired many spike substitutions that prevent the binding of antibodies elicited by vaccinations and infections. Notably, the BA.1 Omicron variant that began spreading widely in late 2020 possessed ~32 spike amino acid substitutions compared to the ancestral SARS-CoV-2 strain (Mannar et al., 2022), leading to an increase in 'breakthrough' infections of vaccinated individuals (Accorsi et al., Altarawneh et al., Cao et al., Kuhlmann et al., 2022; Levin et al., 2021; Pulliam et al., 2022).

Omicron breakthrough infections induce efficient anamnestic immune responses that recruit memory T and B cells cross-reactive to the ancestral strain (Addetia et al., 2023; Kared et al., Koutsakos et al., 2022; Painter et al., 2023; Park et al., Wang et al., 2022; Weber et al., Yisimayi et al., 2023). Many unanswered questions remain on how initial SARS-CoV-2 encounters affect the specificity of antibodies elicited against variant viral strains. For example, bivalent boosters containing BA.5 spike elicit B cell and antibody responses cross-reactive to the ancestral SARS-CoV-2 strain in individuals who received ancestral mRNA-LNP vaccines (Addetia et al., 2023), but this 'immunological imprinting' effect may be less pronounced in individuals who initially received inactivated vaccines (Yisimayi et al., 2023). It remains unclear if repeat exposures with SARS-CoV-2 variants can overcome memory B cell biases established by initial SARS-CoV-2 encounters (Addetia et al., Alsoussi et al., Schiepers et al., Yisimayi et al., 2023). Further, it is unknown if variants with larger antigenic distances are better able to stimulate *de novo* responses while recalling fewer memory B cells in individuals who received ancestral mRNA-LNP vaccines.

Here, we elucidated the specificity of antibody and B cell responses elicited by BA.5 and XBB exposures in individuals previously vaccinated with mRNA-LNPs expressing the ancestral SARS-CoV-2 spike. We compared immune responses in individuals with different amounts of cross-reactive B cells and antibodies at time of variant exposure. We used antigen-specific flow cytometric analyses to interrogate spike-specific B cell responses and performed enzyme-linked immunosorbent assays (ELISAs), neutralization assays, and absorption assays to characterize SARS-CoV-2 reactive antibodies.

Results

BA.5 breakthrough infections elicit antibodies that cross-react to ancestral SARS-CoV-2

To better understand the specificity and functionality of antibodies elicited by breakthrough infections, we characterized antibodies in sera collected from individuals (n=8) who received 3 doses of mRNA-LNP vaccines expressing the ancestral spike and were subsequently infected with a BA.5 Omicron variant in 2022 (breakthrough infections occurred on average 291 days since last vaccination; Painter et al., 2023) (**Figure 1A**). Sera were collected at baseline ~0-5 days (T1) and ~45 days (T2) after BA.5 breakthrough infection. We first quantified serum antibodies reactive to full length spike proteins from the ancestral virus, the breakthrough variant (BA.5), and a variant from 2023 that did not yet exist at the time of sample collection (XBB.1.5). Antibodies reactive to all 3 spike proteins increased >2 fold after BA.5 breakthrough infection (**Figure 1B**). Similar increases were observed when we measured antibodies reactive to the receptor binding domain (RBD) of the spike protein from the ancestral, BA.5, and XBB.1.5 viruses, with the largest fold increase to BA.5 RBD (**Figure 1C**). Prior to breakthrough infection, most participants had high neutralizing antibodies against ancestral SARS-CoV-2, but low or undetectable levels of neutralizing antibodies against BA.5 and XBB.1.5 (**Figure 1D**). Neutralizing antibodies against ancestral SARS-CoV-2 and the BA.5 variant were boosted upon BA.5 variant breakthrough infection in most participants, whereas neutralizing antibodies

against XBB.1.5 were minimally boosted and remained low after infection (**Figure 1D**). This led to an observed increase in antibody neutralization potency (the neutralizing antibody titer divided by total spike targeting antibody titer) for ancestral SARS-CoV-2 and BA.5, but not XBB.1.5 (**Figure 1E**). Thus, BA.5 breakthrough infections elicited neutralizing antibodies against ancestral SARS-CoV-2 and BA.5, but these antibodies poorly neutralized the XBB.1.5 variant that did not yet exist at the time of infection.

Given that we observed simultaneous increases in neutralizing antibodies reactive to the ancestral SARS-CoV-2 virus and BA.5 variant, we hypothesized that BA.5 breakthrough infections elicit neutralizing antibodies that recognize epitopes conserved between these viruses. To address this, we performed ELISAs and neutralization assays with sera that were previously absorbed with carboxyl-magnetic beads coupled with different spike proteins. In these assays (Anderson et al., 2022; Arevalo et al., 2020), antibodies that bind to the spike-coupled beads are removed and unbound antibodies are then assessed for reactivity against different antigens (**Figure S1A**). As expected, beads coated with the ancestral SARS-CoV-2 spike were able to remove >99% of antibodies reactive to the ancestral SARS-CoV-2 full length spike and RBD, while beads coated with either BA.5 or XBB.1.5 spikes reduced but did not entirely remove these antibodies (**Figure 1F-G**). Consistent with this observation, sera absorbed with beads coated with the ancestral SARS-CoV-2 spike could no longer neutralize ancestral SARS-CoV-2, while sera absorbed with beads coated with either the BA.5 or XBB.1.5 spike still contained antibodies capable of neutralizing the ancestral strain (**Figure 1H**). Conversely, beads coated with either the ancestral SARS-CoV-2 spike or BA.5 spike efficiently removed antibodies that bound (**Figure 1I-J**) and neutralized (**Figure 1K**) BA.5 virus, suggesting that nearly all BA.5-reactive antibodies elicited by BA.5 breakthrough infections cross-react to the ancestral SARS-CoV-2 spike. Throughout these studies, it became apparent that some of these ancestral/BA.5 cross-reactive antibodies recognize epitopes that are altered in XBB.1.5, since

serum pre-incubation with beads coated with the XBB.1.5 spike did not eliminate binding (~20% remaining, **Figure 1I-J**) or neutralization (~40% remaining, **Figure 1K**) of BA.5. These data, combined with overall low XBB.1.5 titers (**Figure 1D, S1B-D**) suggest that BA.5 breakthrough infections elicit antibodies that cross-react with the ancestral SARS-CoV-2 and BA.5 spikes, and that substitutions in the XBB.1.5 variant prevent binding of a fraction of these antibodies, especially neutralizing antibodies.

A second BA.5 exposure elicits antibodies that cross-react to ancestral SARS-CoV-2

We next analyzed sera from an additional 9 individuals who received 3 doses of an mRNA-LNP vaccine expressing the ancestral SARS-CoV-2 spike who were later exposed twice to BA.5 through sequential infections and vaccinations (**Figure 2A**). These individuals received a dose of bivalent ancestral/BA.5 spike mRNA-LNP vaccine either before (n=4) or after (n=5) experiencing a BA.5 breakthrough infection. Sera were collected early (~0-5 days, T1) and ~45 days (T2) after the second BA.5 exposure, which occurred on average 76 days (27-156) after the first BA.5 exposure. Antibodies reactive to the ancestral, BA.5, and XBB.1.5 spike proteins were high prior to the second BA.5 exposure and were minimally boosted (**Figure 2B-C**). Most individuals had high baseline neutralizing antibodies against both ancestral SARS-CoV-2 and BA.5 and these antibodies were minimally boosted upon second BA.5 exposure (**Figure 2D**). Neutralizing antibody titers against the XBB.1.5 variant were low in most individuals both before and after the second BA.5 exposure (**Figure 2D**). We observed a modest decrease in serum neutralization potency for all variants tested after secondary BA.5 exposure (**Figure 2E**). Antibody responses were similar regardless of whether the first or second BA.5 exposure was via infection or vaccination (**Figure S2A-C**).

We performed additional absorption assays and found that, similar to antibodies elicited by single BA.5 breakthrough infections, BA.5-reactive antibodies from individuals exposed twice

with BA.5 bound to the ancestral SARS-CoV-2 spike, but only partially recognized the XBB.1.5 spike (**Figure 2F-K, S2D-F**). Thus, antibodies elicited by a second BA.5 spike exposure did not target BA.5-specific epitopes, but instead recognized epitopes conserved in the ancestral spike that became mutated in the XBB.1.5 variant.

Cross-reactive B cell responses dominate first and second BA.5 exposures in individuals previously vaccinated with mRNA-LNP vaccines expressing the ancestral spike

We hypothesized that cross-reactive antibodies in our study were likely produced by B cells generated after the initial exposures to the ancestral spike and subsequently recalled in response to first and second BA.5 exposures. To measure levels of cross-reactive B cells elicited by first and second BA.5 exposures, we performed a flow cytometric B-cell antigen probe assay using PBMCs collected from participants at timepoints corresponding to our serological assays (**Fig. 3A, S3**). We quantified B cells that recognized the RBD of ancestral, BA.5, and XBB.1.5 spike proteins. Following first BA.5 exposures, the proportion of ancestral RBD-binding B cells that also bound BA.5 RBD increased in most individuals, and these responses did not greatly increase following a second BA.5 exposure (**Fig. 3B**). In further accordance with our serological data, XBB.1.5 cross-reactivity was only observed in a fraction of BA.5-binding B cells at all timepoints, and XBB.1.5 cross-reactivity did not increase following BA.5 infection (**Fig. 3C-D**). We did not observe robust variant-specific B cell responses, as extremely low frequencies of B cells bound BA.5 or XBB.1.5 RBD without binding ancestral RBD (BA.5-specific and XBB.1.5-specific, respectively), and the frequency of BA.5-only and XBB.1.5-only B cells did not increase following BA.5 exposure (**Fig. 3E-F**). Together, these data demonstrate that ancestral cross-reactive B cells are stimulated upon BA.5 exposure, leading to a heavily cross-reactive antibody response with no detectable production of antibodies that target novel epitopes on the RBD of the BA.5 spike.

BA.5 exposures elicit antibodies targeting conserved RBD residues mutated in XBB.1.5

Our data suggest that BA.5 exposures boost antibodies that target spike residues that are conserved between ancestral and BA.5 variants but are mutated in XBB.1.5. To map the specificity of these antibodies, we completed additional absorption assays with BA.5 spike proteins that were engineered to possess different RBD amino acid substitutions. We absorbed serum samples with BA.5 spike mutants that had one or two XBB.1.5 RBD amino acid substitutions at residues that are shared between ancestral and BA.5 spikes but differ in XBB.1.5 (spike amino acid residues 346, 368, 445/446, 460, and 490) (**Figure 4A)**. We also absorbed serum with 7 additional BA.5 spike proteins with different combinations of XBB.1.5 RBD mutations, including a mutant that possessed all RBD substitutions that are shared between ancestral and BA.5 spikes but differ in XBB.1.5 spike (protein M7, **Figure 4B)**. Absorption with BA.5 spikes with each single substitution decreased the ability of serum antibodies to bind wildtype BA.5, suggesting that a fraction of polyclonal antibodies targeted each mutated site (**Figure 4C**). Absorption with BA.5 proteins with multiple mutations further decreased the binding of BA.5-reactive antibodies (**Figure 4C**). Similar results were obtained when we repeated experiments with sera isolated from ancestral vaccinated individuals after two BA.5 exposures (**Figure 4D**). Sera absorbed with the M7 protein containing all XBB.1.5 RBD substitutions efficiently neutralized BA.5, indicating that a large fraction of BA.5 neutralizing antibodies targeted epitopes that are conserved between the ancestral and BA.5 RBDs but not the XBB.1.5 RBD (**Figure 4E, F, S4**). Collectively, these data support the hypothesis that BA.5 exposures elicit antibodies that target epitopes conserved in the ancestral spike RBD that later became mutated in the XBB.1.5 variant.

XBB exposures elicit antibodies cross-reactive to the ancestral spike in individuals previously vaccinated with mRNA-LNP vaccines expressing the ancestral spike

XBB, the recombinant variant of BA.2.10.1 and BA.2.75 sublineages containing ~43 spike mutations, and its subvariants, namely XBB.1.5, have dominated infections since late 2022 and resulted in a shift to a new monovalent booster vaccine in September 2023 (CDC, Selvavinayagam et al., Wang et al., 2023; WHO 2022). We longitudinally sampled individuals who were exposed to XBB.1.5 via the monovalent mRNA-LNP booster (n = 12) or by XBB-subvariant breakthrough infections (symptom onset between 1/2/2022 and 10/1/2022, n = 10) and assessed the specificity and functionality of antibody and B cell responses (**Figure 5A**). We observed a robust increase in antibodies that bound and neutralized the ancestral and XBB.1.5 variant 15 and 45 days after XBB.1.5 monovalent mRNA-LNP vaccination or XBB.1.5 infection (**Figure 5B-D)**. While increases in antibody titers to both viruses were significant, the fold-increase in XBB.1.5 neutralizing titers was ~5-fold higher than that of ancestral strain, and neutralization potency of XBB.1.5 antibodies increased slightly following XBB.1.5 exposure, whereas that of ancestral did not (**Figure 5D-E**). We found that XBB.1.5 monovalent mRNA-LNP vaccination rapidly boosted XBB.1.5 neutralizing antibodies that peaked 15 days after vaccination, whereas antibodies elicited by XBB.1.5 infections steadily rose for 45 days after exposure, consistent with earlier reports of slower kinetics of immune responses elicited by breakthrough infections (Koutsakos et al., 2022; Painter et al., 2023) (**Figure S5A-C)**. Although early kinetics differed, antibodies elicited by XBB.1.5 infections and vaccinations were at similar levels by 45 days after exposure (**Figure S5A-C**).

We performed absorption assays using sera collected 45 days after XBB.1.5 exposures to identify antibody specificities elicited by XBB infections and monovalent vaccinations. Beads coated with the XBB.1.5 spike poorly absorbed antibodies that bound (**Figure 5F**) and neutralized (**Figure 5G**) the ancestral SARS-CoV-2 strain. Conversely, beads coated with the ancestral spike absorbed most XBB.1.5-reactive and neutralizing antibodies (**Figure 5H-I, S5E**), suggesting that the majority of antibodies elicited by XBB exposures bound to epitopes

conserved in the ancestral spike. While most individuals produced XBB.1.5-reactive antibodies that targeted epitopes conserved in the ancestral spike, we identified some individuals who produced XBB.1.5-specific responses that were only partially absorbed by beads coated with the ancestral spike (**Figure 5H-I, S5E**). These data suggest that XBB.1.5, which is more antigenically distant compared to BA.5, is capable of eliciting variant-specific responses in a subset of individuals who were previously vaccinated with mRNA-LNP expressing the ancestral spike.

Next, we characterized antibodies in sera from 3 individuals who were infected with an XBB-variant and subsequently received the XBB.1.5 monovalent booster (average 139 days after infection, **Figure 5J**). Unlike a second BA.5 exposure, a second XBB exposure greatly increased XBB.1.5 neutralizing antibody titers and potency (**Figure 5K, S5F-H)**. Using absorption assays, we also observed increases in both XBB.1.5-specific binding and neutralizing antibodies following the second XBB exposure (**Figure 5L-N, S5I-K)**. Similar to single XBB exposures, the majority of neutralizing antibodies elicited by two XBB exposures targeted epitopes in the ancestral spike, with XBB.1.5-specific antibodies constituting only 17% of total XBB.1.5 neutralizing antibodies. Nonetheless, these experiments demonstrate that XBB can provoke variant-specific responses in a subset of individuals who previously received mRNA-LNP vaccines expressing the ancestral spike, and that these responses can be further boosted by sequential XBB exposures.

Cross-reactive B cell responses dominate following XBB exposures in individuals previously vaccinated with mRNA-LNP vaccines expressing the ancestral spike

To further explore the relationships between cross-reactive and variant-specific responses elicited by XBB, we analyzed antigen-specific B cells elicited after XBB exposures. We observed a significant increase in ancestral and XBB.1.5-reactive B cells by 15 days post-

exposure, followed by a slight contraction by day 45 (**Fig 6A-B)**. The percent of ancestral RBD-binding B cells that were cross-reactive with XBB.1.5 increased significantly by day 7 and remained above baseline at day 45 (**Fig. 6C**). The frequencies of XBB.1.5-specific B cells (cells that did not cross-react with ancestral RBD) were low but significantly expanded between days 0 and 7 before contracting by day 45 (**Fig. 6D, Fig. S6A**). There was substantial heterogeneity in the magnitude of XBB.1.5-specific B cell expansion, suggesting that variant-specific responses may be restrained in some individuals (**Fig. 6D**). Despite expanding significantly during acute XBB exposures, the proportion of XBB.1.5 RBD-binding B cells that were specific for XBB.1.5 did not increase, consistent with the cross-reactive response remaining dominant compared to variant-specific responses (**Fig. 6E**).

CD71 is expressed following B cell activation, with reactivated memory B cells expressing higher CD71 than stimulated naïve B cells (Auladell et al., 2019). CD71 was rapidly upregulated after XBB exposure and was significantly elevated on XBB.1.5 cross-reactive and XBB.1.5-specific B cells at day 7 and day 15 compared to bulk B cells or B cells that bound the ancestral RBD but not the XBB.1.5 RBD (**Fig. 6F-G, S6B**). XBB.1.5-specific B cells expressed lower CD71 than XBB.1.5 cross-reactive B cells, consistent with differences between recall responses from memory B cells and *de novo* responses arising from naïve B cells (Auladell et al., 2019). XBB.1.5 cross-reactive B cells were class-switched and expressed IgG, whereas most XBB.1.5-specific B cells were not class-switched to IgA or IgG (**Fig. 6H**), suggesting that they were likely derived from *de novo* responses. In addition to rapid CD71 upregulation, XBB.1.5-binding plasmablasts, including XBB.1.5-specific plasmablasts, increased dramatically by day 7 after XBB.1.5 exposure (**Fig 6I-J**). Taken together, these data suggest that XBB elicits a potent B cell response that is largely cross-reactive with the ancestral spike, with some individuals generating variant-specific B cells.

Finally, we wanted to determine what cellular or serological metrics were associated with the production of XBB.1.5-specific responses. Elevated baseline antibody titers, ancestral and XBB.1.5 RBD-binding B cell frequencies, and XBB.1.5 cross-reactive B cell frequencies were all associated with diminished XBB.1.5-specific B cell responses (**Fig. 6K, S6C-D**). Moreover, high pre-existing antibody titers against XBB.1.5 spike were associated with decreased XBB.1.5-specific neutralizing antibody titers (**Fig. 6L**). As expected, there was a positive correlation between XBB.1.5-specific B cells at day 7 and peak XBB.1.5-specific neutralizing antibody titers (**Fig. 6L**). XBB.1.5-specific antibodies were also correlated with XBB.1.5-specific B cell expansion and the percent of XBB.1.5-binding B cells that were XBB.1.5-specific (**Fig. S6E**). Together, these analyses support a model in which pre-existing B cells and antibodies influence the development of variant-specific responses, where individuals with lower pre-existing antibody titers and fewer cross-reactive memory B cells are better able to activate naïve XBB.1.5-specific B cells and produce XBB.1.5-specific antibodies. However, baseline cross-reactive B cells are strongly correlated with peak XBB.1.5 neutralizing antibody titers, whereas XBB.1.5-specific B cell responses have no association with overall XBB.1.5 neutralizing antibody titers after infection or vaccination (**Fig. 6M**). This is consistent with the observation that the majority of XBB.1.5 neutralizing antibodies cross-react to the ancestral spike. Overall, these analyses highlight the diversity of the humoral response to XBB and define several key factors contributing to the development of variant-specific B cells and antibodies.

Discussion

Through longitudinal sampling and intensive serological and cellular analyses, our studies demonstrate that B cells elicited by ancestral SARS-CoV-2 mRNA vaccines are efficiently recalled by SARS-CoV-2 variants, leading to the rapid production of neutralizing antibodies against epitopes conserved between ancestral and variant strains. We found that the BA.5 spike elicits antibodies that recognize epitopes conserved between the ancestral and BA.5 spikes, but

fail to bind to the more antigenically distant XBB.1.5 spike. Similarly, the majority of antibodies elicited by XBB infection or monovalent vaccination targeted epitopes conserved between the ancestral and XBB.1.5 spikes. Both BA.5 and XBB elicited responses that were dominated by memory B cells primed by prior ancestral mRNA-LNP vaccinations; however, unlike BA.5, we found that XBB elicited low levels of variant-specific B cell and antibody responses in some individuals.

Our data are consistent with reports showing antibody responses to SARS-CoV-2 variants typically cross-react to the ancestral spike in individuals who initially encountered ancestral SARS-CoV-2 antigens (Addetia et al., Chalkias et al., 2023; Kared et al., Koutsakos et al., 2022; Painter et al., 2023; Park et al., 2022; Tortorici et al., 2023; Wang et al., 2022; Wang et al., Weber et al., Yisimayi et al., 2023). Clinical studies have shown that BA.5 and XBB.1.5 variant booster vaccines are highly effective at reducing deaths and hospitalizations caused by circulating variants (Carr et al., Hoffmann et al., Lin et al., Lin et al., Shresta et al., Tan et al., Tan et al., Wang et al., 2023). It is likely that antibodies targeting epitopes conserved with the ancestral SARS-CoV-2 spike contribute to variant booster vaccine protection. It is important to highlight that cross-reactive B cells elicited by earlier ancestral SARS-CoV-2 mRNA-LNP vaccinations are strongly correlated with the induction of high levels of XBB.1.5 neutralizing antibodies after monovalent XBB.1.5 vaccination. Therefore, while ‘immune imprinting’ by ancestral SARS-CoV-2 mRNA-LNP vaccines clearly influence the specificity of antibodies elicited by variant infections and vaccinations, these prior vaccinations are also highly beneficial for establishing memory B cells that can be rapidly recruited to produce neutralizing antibodies against SARS-CoV-2 variants.

Further studies should evaluate if SARS-CoV-2 antigens with greater antigenic distances are able to efficiently elicit variant-specific *de novo* antibody responses in individuals who were

346 previously vaccinated with ancestral mRNA-LNP vaccines. In our studies, XBB exposures
347 promoted the development of low-level variant-specific XBB.1.5-specific antibody responses in
348 some individuals. These variant-specific responses were associated with lower baseline SARS-
349 CoV-2 XBB.1.5-specific antibody titers and B cell frequencies, suggesting that factors such as
350 epitope masking and feedback inhibition may potentially limit the recruitment of naïve B cells
351 that target novel epitopes on variant spike proteins (Bergström et al., 2017; Schaefer-Babajew
352 et al., 2023; Tas et al., 2022). It will also be important to quantify the level of somatic
353 hypermutation in B cells that produce antibodies that bind specifically to variants. While it is
354 likely that variant-specific antibodies in our studies are derived from *de novo* activated B cells, it
355 is also possible that these antibodies are produced from memory B cells that have lost binding
356 to ancestral spike through somatic hypermutation.
357
358 Future studies should also determine if mRNA-LNP and inactivated virus vaccines elicit different
359 'immunological imprints' that affect the specificity and magnitude of antibody responses elicited
360 by variant infections and vaccinations. Comparative analyses have previously focused on
361 general immunogenicity and effectiveness against severe disease, showing higher antibody
362 titers and better overall protection in mRNA-LNP vaccinated individuals compared to inactivated
363 virus vaccinated individuals (Lim et al., 2021, Premikha et al., 2019), Yisimayi and colleagues
364 recently demonstrated that individuals who previously received inactivated SARS-CoV-2
365 vaccine produced robust variant-specific responses after subsequent Omicron exposures
366 (Yisimayi et al., 2023). Taken with our data and others, this suggests that inactivated virus
367 vaccines potentially establish weaker 'immunological imprints' compared to mRNA-LNP
368 vaccines.
369
370 The human immune landscape against SARS-CoV-2 is becoming more heterogenous as
371 variants emerge and infection and vaccination histories become diverse among different

372 individuals. Most humans have been 'immunologically imprinted' with antigens from the
373 ancestral SARS-CoV-2 strain, but that will inevitably change as time progresses. Most children
374 born today will be first introduced to SARS-CoV-2 antigens in the form of a variant infection or
375 variant vaccination, leading to the formation of different memory B cell populations compared to
376 individuals first exposed to ancestral SARS-CoV-2 antigens. Though the impact of birth year
377 imprinting on the evolution of future SARS-CoV-2 variants is unknown, there is evidence of
378 influenza epidemic virus susceptibilities being shaped by childhood exposures (Arevalo et al.,
379 2020; Gostic et al., 2016; Gostic et al., 2019). Overall, an improved understanding of how
380 SARS-CoV-2 immune history influences antibody specificity to new variants will be critical for
381 rationally designing future vaccines and mitigating disease burden.
382
383 **Limitations of this study**
384 While most individuals in these cohorts followed a similar 3-dose vaccination with mRNA-LNP
385 expressing the ancestral spike followed by BA.5 breakthrough infection, some individuals
386 experienced infections with prior variants, as shown in **Supplemental Table 1**. The XBB cohort
387 included individuals with a more diverse exposure history. We did not follow a single longitudinal
388 cohort of individuals following first and second BA.5 exposures and through subsequent
389 XBB.1.5 vaccinations, which introduces variance between all cohorts. Our antibody functionality
390 assays were limited to pseudovirus neutralization assays, which have been shown to be highly
391 correlative with live virus neutralization assays. For our BA.5 cohorts, we only measured
392 functionality of antibodies at two timepoints and specificity at a single timepoint; it is possible
393 epitope targeting continues to change over time after antigen exposure. Additional analyses of
394 late timepoints will be important to include in future studies to understand how antibody
395 specificities change over time.
396
397

Acknowledgements

We would like to thank the study participants for their generosity in making the study possible. We also thank the Penn Cytomics and Cell Sorting Resource Laboratory for access to instruments, members of the Hensley and Wherry labs for helpful discussions and feedback, and the Immune Health team. This project has been funded in part with Federal funds from the National Institute of Allergy and Infectious Diseases, National Institutes of Health, Department of Health and Human Services, under Contract No. 75N93021C00015 (S.E.H. and E.J.W.) and Grant Nos. U19AI082630 (S.E.H. and E.J.W.), AI105343 (E.J.W.), AI108545 (E.J.W.), AI155577 (E.J.W.), AI149680 (E.J.W.); and the Parker Institute for Cancer Immunotherapy (to EJW). S.E.H. holds an Investigators in the Pathogenesis of Infectious Disease Awards from the Burroughs Wellcome Fund. D.B.R. was supported by an MD fellowship of the Boehringer Ingelheim Fonds.

Author Contributions

Conceptualization, T.S.J., M.M.P., E.J.W., and S.E.H.; Methodology, T.S.J., S.H.L., and M.M.P.; Investigation, T.S.J., S.H.L., R.K.A., N.R.D., D.B.R., and M.M.P.; Formal Analysis, T.S.J. and M.M.P.; Visualization, T.S.J. and M.M.P.; Writing – Original Draft, T.S.J. and S.E.H., Writing – Review & Editing, T.S.J., S.H.L., M.M.P., E.J.W., D.C.D., and S.E.H.; Supervision, D.C.D, E.J.W., and S.E.H.; Funding Acquisition, E.J.W. and S.E.H.; Resources, E.J.W. and S.E.H.

Declaration of Interests

E.J.W. is a member of the Parker Institute for Cancer Immunotherapy. E.J.W. is an advisor for Arsenal Biosciences, Coherus, Danger Bio, IpiNovyx, Janssen, New Limit, Marengo, Pluto Immunotherapeutics Related Sciences, Santa Ana Bio, and Synthekine. E.J.W. is a founder of and holds stock in Coherus, Danger Bio, and Arsenal Biosciences.

Inclusion and Diversity

We support inclusive, diverse, and equitable conduct of research.

Figure Legends

Figure 1. BA.5 breakthrough infection elicits cross-reactive antibodies evaded by XBB.1.5.

A) Schematic of participants in this study who were vaccinated 3x with the SARS-CoV-2 ancestral mRNA-LNP vaccine who then had a BA.5 breakthrough infection. B)-C) Antigen-specific IgG ELISAs were performed using sera from timepoints indicated in panel A) against ancestral, BA.5, and XBB.1.5 full-length spike (B) and RBD (C) proteins. Endpoint titers are reported as reciprocal serum dilutions. D) SARS-CoV-2 pseudotype neutralization assays were performed using sera obtained at timepoints indicated in panel A) against ancestral SARS-CoV-2, BA.5, and XBB.1.5 pseudoviruses. Values reported are focus reduction neutralization test (FRNT) 50, or reciprocal serum dilution at which <50% viral input foci are observed. E) Neutralization potency was calculated by dividing FRNT50 values by spike IgG titer. F-G) Antigen-specific IgG ELISAs were performed using T2 absorbed sera and ELISA plates coated with the ancestral spike (F) or ancestral RBD (G). H) SARS-CoV-2 pseudotype neutralization assays were performed using T2 absorbed serum and ancestral SARS-CoV-2 pseudovirus. I-J) Antigen-specific IgG ELISAs were performed using T2 absorbed and ELISA plates coated with BA.5 spike (I) and BA.5 RBD (J). K) Neutralization assays were performed using T2 absorbed serum and BA.5 pseudotyped virus. For all, individual points are average of n = 2 technical replicates. Red/black bars indicate geometric mean. Wilcoxon signed-rank test with benjamini-hochberg correction for multiple testing. All comparisons to timepoint 1 or mock absorption. * $p<0.05$, ** $p<0.01$.

Figure 2. Secondary BA.5 exposure elicits cross-reactive antibodies that bind weakly to XBB.1.5.

A) Schematic of participants in this study who were vaccinated 3x with the SARS-CoV-2 ancestral mRNA-LNP vaccine who then had two BA.5 exposures. B)-C) Antigen-specific IgG ELISAs were performed using sera from timepoints indicated in panel A) against ancestral,

BA.5, and XBB.1.5 full-length spike (B) and RBD (C). Endpoint titers are reported as reciprocal dilutions. D) SARS-CoV-2 pseudotype neutralization assays were performed using sera obtained at timepoints indicated in panel A) against ancestral SARS-CoV-2, BA.5, and XBB.1.5 pseudoviruses. Values reported are focus reduction neutralization test (FRNT) 50, or reciprocal serum dilution at which <50% viral input foci are observed. E) Neutralization potency was calculated by dividing FRNT50 values by spike IgG titer. F)-G) Antigen-specific IgG ELISAs were performed using T2 absorbed sera and ELISA plates coated with the ancestral spike (F) or ancestral RBD (G). H) SARS-CoV-2 pseudotype neutralization assays were performed using T2 absorbed serum and ancestral SARS-CoV-2 pseudovirus. I-J) Antigen-specific IgG ELISAs were performed using T2 absorbed sera and ELISA plates coated with BA.5 spike (I) and BA.5 RBD (J). K) Neutralization assays were performed using T2 absorbed serum and BA.5 pseudotyped virus. For all, Individual points are average of n = 2 technical replicates. Red/black bars indicate geometric mean. Wilcoxon signed-rank test with benjamini-hochberg correction for multiple testing. All comparisons to timepoint 1 or mock absorption. * $p<0.05$, ** $p<0.01$.

Figure 3. Cross-reactive B cells are recruited in response to primary and secondary BA.5 exposures in vaccinated individuals. A) Representative flow-cytometry plot showing gating strategy for probe positive memory B cells. B) The percent of ancestral RBD-binding B cells that cross-bind to BA.5 RBD before and after first (left) and second (right) exposure to BA.5. C) The percent of ancestral RBD and BA.5 RBD cross-binding B cells that also cross-bind to XBB.1.5 RBD before and after first (left) and second (right) exposure to BA.5. D) The percent of ancestral RBD-binding B cells that cross-bind BA.5 and XBB.1.5 RBD before and after first (left) and second (right) exposure to BA.5. E-F) The frequency of BA.5 RBD-binding (E) and XBB.1.5 RBD-binding (F) B cells that do not cross-react with ancestral RBD before and after first (left) and second (right) exposure to BA.5.

Figure 4. Antibodies elicited by successive ancestral SARS-CoV-2 and BA.5 exposures target conserved residues that are mutated in the XBB.1.5 RBD. A) Ancestral RBD structure with residues that are different in BA.5 are highlighted in purple, and residues conserved between ancestral and BA.5 but different in XBB.1.5 are highlighted in teal (PDB 6M0J). B) List of recombinant mutations created for this study using the BA.5 spike backbone. C) IgG ELISA using T2 breakthrough sera after absorption with single mutants and those listed in panel B. D) IgG ELISA usingT2 sera from individuals exposed twice with BA.5 after absorption with single mutants and those listed in panel B. E,F) Neutralization assays were performed using T2 absorbed serum from single (E) and two (F) BA.5 exposures using BA.5 pseudotype virus. For all, individual points are average of n = 2 technical replicates. Black bars indicate geometric mean. Wilcoxon signed-rank test with benjamini-hochberg correction for multiple testing. All comparisons to mock absorption. * $p<0.05$, ** $p<0.01$.

Figure 5. Primary and secondary XBB exposures elicit mostly antibodies that cross-react to the ancestral SARS-CoV-2 spike. A) Schematic of participants in this study who were exposed to XBB. B)-C) Antigen-specific IgG ELISAs were performed using sera from timepoints indicated in panel A) against ancestral and XBB.1.5 full-length spike (B) and RBD (C). Endpoint titers are reported as reciprocal dilutions. D) Neutralization assays were performed using serum obtained at timepoints indicated in panel A) against ancestral and XBB.1.5 SARS-CoV-2 pseudoviruses. Values reported are focus reduction neutralization test (FRNT) 50, or reciprocal serum dilution at which <50% viral input foci are observed. E) Neutralization potency was calculated by dividing FRNT50 values by spike IgG titer. F),H) Antigen-specific IgG ELISAs were performed using sera (collected 45 days after XBB1.5 exposure) after absorption with ancestral or XBB.1.5 spike proteins. G),I) SARS-CoV-2 pseudotype neutralization assays were performed using sera (collected 45 days after XBB.1.5 exposure) after absorption with ancestral or XBB.1.5 spike proteins. J) Schematic of participants in this study who were exposed twice to XBB. K) SARS-

CoV-2 pseudotype neutralization assays were performed using sera obtained at timepoints indicated in panel J) using ancestral and XBB.1.5 pseudoviruses. L),M) Antigen-specific IgG ELISAs and N) SARS-CoV-2 neutralization assays were performed using sera (collected 45 days after each XBB.1.5 exposure) after absorption with ancestral or XBB1.5 spike proteins. For all, Individual points are average of n = 2 technical replicates. Red/black bars indicate geometric mean. Wilcoxon rank-sum test with benjamini-hochberg correction for multiple testing. All comparisons to timepoint 1 or mock absorption. * $p<0.05$, ** $p<0.01$, *** $p<0.001$, **** $p<0.0001$.

Figure 6. Cross-reactive B cells dominate immune responses elicited by XBB, but variant-specific responses are observed in individuals with low pre-existing immunity. A-B) The percent of total B cells that bind A) ancestral RBD and B) XBB.1.5 RBD before and after exposure to XBB.1.5. C) The percent of ancestral RBD-binding B cells that cross-bind to XBB.1.5 RBD before and after exposure to XBB.1.5. D) The fold expansion of B cells that bind XBB.1.5 RBD but not ancestral RBD (XBB.1.5-specific) following XBB.1.5 exposure. E) The percent of total XBB.1.5 RBD-binding B cells that do not bind ancestral RBD. F) Representative flow cytometry plots depicting longitudinal changes in CD71 expression on different RBD-binding B cell populations from a single individual. G) Summary data of median CD71 expression on the indicated RBD-binding B cell populations at 0, 7, 15, and 45 days post-XBB exposure. H) Summary data of the isotype distribution of RBD-binding B cells at 0, 7, 15, and 45 days post-XBB exposure. I-J) The percent of total B cells that are CD38+CD27+ plasmablasts and I) bind XBB.1.5 RBD or J) bind XBB.1.5 RBD and do not bind ancestral RBD (XBB.1.5-specific). K-M) Correlations within B cell and antibody responses. K) Correlation of day 7 fold change in XBB.1.5-specific B cells as in panel D with day 0 percent of total B cells that bind ancestral RBD (left); day 0 percent of total B cells that bind XBB.1.5 RBD (center); day 0 XBB.1.5 spike-binding antibodies by ELISA (right). L) Correlations of ancestral spike absorbed XBB.1.5 neutralizing antibody titers at day 45 (as in Fig. 5N) with day 0 XBB.1.5 spike-binding antibodies quantified

by ELISA (left), and the percent of total B cells that bind XBB.1.5 RBD but not ancestral RBD at day 7 (right). M) Correlation of overall day 45 XBB.1.5 neutralizing antibody titers (unabsorbed) with the day 0 percent of ancestral RBD+ B cells that cross-bind XBB.1.5 RBD; the day 15 percentage of total B cells that bind XBB.1.5 RBD, the day 15 percentage of total B cells that bind XBB.1.5 RBD but do not bind ancestral RBD (XB.1.5-specific), and the day 15 fold change in XBB-specific B cells as in D. Points represent individual subjects and thin lines indicate individual subjects sampled longitudinally. Horizontal bars represent means. Statistics were calculated using two-sided Wilcoxon test with Benjamini-Hochberg correction for multiple comparisons. Statistics without brackets are in comparison to day 0. Correlation statistics were calculated using Spearman rank correlation and are shown with Pearson trend lines for visualization.

Methods

Human Subject Recruitment and Sampling

Human subjects were recruited for this study for longitudinal sampling before and after either mRNA booster vaccination or SARS-CoV-2 breakthrough infection (IRB#851465). Full cohort and demographic information are provided in **Supplemental Table 1**. Additional healthy donor PBMC samples were collected with approval from the University of Pennsylvania Institutional Review Board (IRB# 845061). For many individuals, baseline samples were acquired prior to SARS-CoV-2 infection or vaccination but at least 2 months after their most recent infection or vaccine dose. These samples are labeled as day 0 throughout the manuscript. Samples were collected on days 7, 15, and 45 based on the date of booster vaccination or the reported date of first symptom onset (IRB#851465). Prior SARS-CoV-2 infection status was determined by self-reporting. All participants were otherwise healthy, with no self-reported history of chronic health conditions, and none were hospitalized during SARS-CoV-2 infection. Peripheral blood samples (30-100mL) and clinical questionnaire data were collected at each study visit.

Peripheral blood sample processing

Following standard phlebotomy procedures, 30-100mL of venous blood was collected into sodium heparin tubes. Plasma was separated by centrifugation at 1800xg for 15 minutes, aliquoted, stored at −80°C, and heat inactivated for 30 minutes at 56°C prior to binding and neutralizing antibody analyses. After removing plasma, the remaining fractions were diluted with RPMI + 1% FBS + 2mM L-Glutamine + 100 U Penicillin/Streptomycin (R1) to achieve a final volume double that of the original whole blood. The diluted blood was then layered over 15mL lymphoprep gradients (STEMCELL Technologies) in SEPMATE tubes (STEMCELL Technologies) and spun at 1200g for 10 minutes. The peripheral blood mononuclear cell (PBMC) fraction was harvested from SEPMATE tubes, washed once with R1 and pelleted, and

cell pellets were resuspended in ACK lysis buffer (Thermo Fisher). After 5 minutes of red blood cell lysis at room temperature, the lysis was quenched by adding R1. PBMCs were then filtered through a 70µm cell strainer and counted using a Countess automated cell counter (Thermo Fisher). Aliquots containing 10×10^6 PBMCs were cryopreserved in 90% FBS 10% DMSO and stored at −80°C for later flow cytometric analyses.

Recombinant Protein Production and Expression

SARS-CoV-2 full-length spike or RBD plasmids were transfected into 293F cells at 1e6 cells/mL at a 1µg :1mL ratio. Cells were incubated for 6 days (full-length spike) or 4 days (RBD) at 37°C and 150 RPM before purification. To purify, cultures were centrifuged at 3200xg for 6 minutes to clarify supernatant. Ni-NTA resin (Qiagen) was resuspended and 5mL was transferred into a 50mL conical for each flask being purified. Volume was brought to 50mL with sterile PBS and conical tubes were centrifuged for 10 minutes at 3200xg. After centrifugation, excess PBS was removed, and resin was added to clarified supernatant. Resin-supernatant mixtures were incubated for 2 hours at 4°C and 220 RPM. After incubation, resin-supernatant was added to gravity columns (Bio-rad), then washed 4X with wash buffer (50 mM NaHCO3, 300 mM NaCl, 20 mM imidazole, pH 8) and eluted in a total volume of 8 mL elution buffer (50 mM NaHCO3, 300 mM NaCl, 300 mM imidazole, pH 8). Eluted protein was concentrated and PBS buffer exchanged using 10kDa (RBD) or 30kDa (full-length spike) centrifugal filters (Sigma-Aldrich). Protein concentrations were measured by BCA assay (ThermoFisher).

Carboxyl-Magnetic Bead Coupling and Serum Absorptions

Recombinant spike proteins were coupled to carboxyl magnetic beads (Ray-biotech) at a ratio of 35 µg antigen to 100 µL beads. The bead-antigen mixture was vortexed then incubated at 4°C with rocking for 2 hours. The unbound fraction was removed by placing beads to a magnetic stand, and beads were quenched by incubating in 50 mM Tris, pH 7.4 for 15 minutes

at RT with rocking. After 15 minutes, beads were placed back on the magnet to remove the quenching buffer. Beads were washed 4x with wash buffer (DPBS supplemented with 0.1% BSA and 0.05% Tween-20). For each wash, 1 bead volume of wash buffer was added to the beads, vortexed, then placed back on the magnet. Beads were finally resuspended in 1 bead-volume of wash buffer before storage at 4°C.

For absorptions, sera were first diluted 1:35.7 with sterile DPBS and then brought to 1:50 dilution with the addition of recombinant protein-coupled beads at a final bead:sera volume ratio of 1:2. The bead-sera mixture was vortexed, then shaken at 1100 RPM for 1 hour at RT. Bead-sera mixtures were then placed on a magnet for separation and unabsorbed fractions were removed and transferred to a clean tube.

Antigen-specific ELISA

Antigen-specific ELISAs were performed as previously described (Anderson et al., 2021). Briefly, high-binding plates (ThermoFisher) were coated with 2 µg/mL of recombinant protein or with DPBS to control for background antibody binding at 4°C overnight. The next day, plates were washed 3x with PBS containing 0.1% Tween 20 (PBS-T) and blocked for 1 hour with 200µL blocking buffer (DPBS supplemented with 3% milk powder and 0.1% tween-20). Plates were then washed 3x with PBS-T, and 50µL serum diluted in dilution buffer (DPBS supplemented with 1% milk and 0.1%Tween-20) were added. After 2 hours of incubation, plates were washed 3x with PBS-T and 50 µL goat anti-human IgG HRP conjugate (Jackson) was added to each well and allowed to incubate for 1 hour. Plates were washed 3x with PBS-T, then 50 µL SureBlue 3,3',5,5'-tetramethylbenzidine substrate (SeraCare) was added to each well. The reaction was allowed to incubate in the dark for 5 minutes before addition of 25 µL 250 mM hydrochloric acid stop solution. Plates were shaken to distribute solution and read at OD450nm immediately using a Spectramax plate reader (Molecular Devices). Serum antibody titers were

obtained from a standard curve of serially diluted pooled serum (starting dilution 1:100). Standard curves were included on all plates for plate-to-plate variation. PBS controls were included for each sample dilution plate to account for nonspecific binding. Antibody titers for each sample were measured in two technical replicates performed on separate days.

SARS-CoV-2 Pseudovirus Production

SARS-CoV-2 pseudotyped vesicular stomatitis virus (VSV) were produced as previously described (Anderson et al., 2021; Goel et al., 2021). Briefly, 293T cells were seeded at 3.5×10^6 cells in collagen-coated 10 cm tissue culture dish, incubated for 24 hours, and transfected using calcium phosphate with 25 µg of SARS-CoV-2 variant plasmids encoding a codon optimized SARS-CoV-2 spike gene with an 18-residue truncation in the cytoplasmic tail. After 24 hours, the SARS-CoV-2 Spike-expressing cells were infected for 2-4 hours with VSV-G pseudotyped VSVΔG-RFP at an MOI of ~2-4. Virus-containing media was removed, and the cells were re-fed with media. VSVΔG-RFP SARS-CoV-2 pseudotypes were harvested 24-28 hours after infection, clarified by centrifugation twice at 6000xg, then aliquoted and stored at −80°C.

Quantification of SARS-CoV-2 pseudotype neutralizing antibody titers

Focus reduction neutralization titers were determined as previously described. Briefly, 96-well collagen-coated plates were seeded with 2.5 x 10^4 TMPRSS2 expressing VeroE6 cells per well the night prior. The next day, heat-inactivated sera or post-absorption sera were serially diluted 2-fold and mixed with 200-300 focus forming units per well of VSVΔG-RFP SARS-CoV-2 pseudotype viruses. Media used for serum and virus dilution contained 600 ng/mL of an anti-VSV-G antibody 1E9F9 to ensure neutralization of any VSV-G carryover virus from pseudotype production. The serum-virus mixture was incubated for 1 hour at 37°C before being plated on VeroE6 TMPRSS2 cells. After 22 hours of incubation at 37°C, plates were washed with DPBS

and fixed with 4% paraformaldehyde. The spots were visualized and counted on an S6 FluoroSpot Analyzer (CTL). The focus reduction neutralization titer 50% (FRNT50) was determined as the greatest serum dilution at which focus count was reduced by at least 50% relative to control wells infected with only pseudotype viruses in the absence of human serum. FRNT50 titers for each sample were measured in two technical.

SARS-CoV-2-specific B cell flow cytometric analyses

Antigen-specific B cells were detected using biotinylated proteins in combination with different streptavidin (SA)–fluorophore conjugates as described (Goel et al., 2021). All reagents are listed in **Supplemental Table 2**. For each sample, biotinylated proteins were multimerized with fluorescently labeled streptavidin (SA) for 1.5 h at 4 °C at the following ratios, all of which are ~4:1 molar ratios calculated relative to the SA-only component irrespective of fluorophore: 200 ng full-length spike protein was mixed with 20 ng SA-BV421, 30 ng NTD was mixed with 12 ng SA-BV786, 25 ng WT RBD was mixed with 12.5 ng SA-PE, 25 ng XBB.1.5 RBD was mixed with 12.5 ng SA-BV711, 25 ng XBB.1.5 RBD was mixed with 12.5 ng SA-PE-Cy7, 25 ng BA.5 RBD was mixed with 12.5 ng SA-BUV615, 25 ng BA.5 was mixed with 12.5 ng SA-APC, 50 ng S2 was mixed with 12 ng SA-BUV737, and 50 ng nucleocapsid protein was mixed with 14 ng SA-BV605. In total, 12.5 ng SA-PE-Cy5 was used as a decoy probe without biotinylated protein to gate out cells that nonspecifically bound SA. All experimental steps were performed in a 50/50 mixture of PBS + 2% FBS and Brilliant buffer (BD Bioscience). Antigen probes were prepared individually and combined after multimerization with 5 μM free D-biotin (Avidity) to minimize potential cross-reactivity between probes. For staining, 2–10 × 10^6 PBMCs per sample were thawed from cryopreservation and prepared in a 96-well round-bottom plate. Cells were first stained with Fc block (BioLegend, 1:200) and Ghost Violet 510 Viability Dye (Tonbo) for 15 min at 4 °C. Cells were then washed and stained for 1 h at 4 °C with 50 μl antigen probe master mix containing the above probes combined immediately before staining. Following this incubation period, cells were

washed again and stained with anti-CD27-BUV395, anti-CD3-BUV563, anti-CD38-BUV661, anti-IgD-BV480, anti-CD19-BV750, anti-IgA-FITC, anti-CD21-PE-CF594, anti-IgG-AF700 and anti-CD71-APC-H7 for 30 min at 4 °C. After surface stain, cells were washed and fixed in 1× Stabilizing Fixative (BD Biosciences) overnight at 4 °C.

Data Analysis

All data were analyzed using Graphpad Prism version 10.1.1 or R version 4.3.2 and visualized using R studio. PyMOL version 2.5.5 was used to visualize ancestral SARS-CoV-2 RBD. Custom R scripts are available upon request.

References

1. Corbett, K.S., Edwards, D.K., Leist, S.R., Abiona, O.M., Boyoglu-Barnum, S., Gillespie, R.A., Himansu, S., Schäfer, A., Ziwawo, C.T., DiPiazza, A.T., Dinnon, K.H., Elbashir, S.M., Shaw, C.A., Woods, A., Fritch, E.J., Martinez, D.R., Bock, K.W., Minai, M., Nagata, B.M., Hutchinson, G.B., Wu, K., Henry, C., Bahl, K., Garcia-Dominguez, D., Ma, L., Renzi, I., Kong, W.-P., Schmidt, S.D., Wang, L., Zhang, Y., Phung, E., Chang, L.A., Loomis, R.J., Altaras, N.E., Narayanan, E., Metkar, M., Presnyak, V., Liu, C., Louder, M.K., Shi, W., Leung, K., Yang, E.S., West, A., Gully, K.L., Stevens, L.J., Wang, N., Wrapp, D., Doria-Rose, N.A., Stewart-Jones, G., Bennett, H., Alvarado, G.S., Nason, M.C., Ruckwardt, T.J., McLellan, J.S., Denison, M.R., Chappell, J.D., Moore, I.N., Morabito, K.M., Mascola, J.R., Baric, R.S., Carfi, A., Graham, B.S., 2020. SARS-CoV-2 mRNA vaccine design enabled by prototype pathogen preparedness. Nature 586, 567–571. https://doi.org/10.1038/s41586-020-2622-0
2. Hsieh, C.-L., Goldsmith, J.A., Schaub, J.M., DiVenere, A.M., Kuo, H.-C., Javanmardi, K., Le, K.C., Wrapp, D., Lee, A.G., Liu, Y., Chou, C.-W., Byrne, P.O., Hjorth, C.K., Johnson, N.V., Ludes-Meyers, J., Nguyen, A.W., Park, J., Wang, N., Amengor, D., Lavinder, J.J., Ippolito, G.C., Maynard, J.A., Finkelstein, I.J., McLellan, J.S., 2020. Structure-based design of prefusion-stabilized SARS-CoV-2 spikes. Science eabd0826. https://doi.org/10.1126/science.abd0826
3. Jackson, L.A., Anderson, E.J., Rouphael, N.G., Roberts, P.C., Makhene, M., Coler, R.N., McCullough, M.P., Chappell, J.D., Denison, M.R., Stevens, L.J., Pruijssers, A.J., McDermott, A., Flach, B., Doria-Rose, N.A., Corbett, K.S., Morabito, K.M., O'Dell, S., Schmidt, S.D., Swanson, P.A., Padilla, M., Mascola, J.R., Neuzil, K.M., Bennett, H., Sun, W., Peters, E., Makowski, M., Albert, J., Cross, K., Buchanan, W., Pikaart-Tautges, R., Ledgerwood, J.E., Graham, B.S., Beigel, J.H., mRNA-1273 Study Group, 2020. An mRNA Vaccine against SARS-CoV-2 - Preliminary Report. N Engl J Med 383, 1920–1931. https://doi.org/10.1056/NEJMoa2022483
4. Mannar, D., Saville, J.W., Zhu, X., Srivastava, S.S., Berezuk, A.M., Tuttle, K.S., Marquez, A.C., Sekirov, I., Subramaniam, S., 2022. SARS-CoV-2 Omicron variant: Antibody evasion and cryo-EM structure of spike protein–ACE2 complex. Science 375, 760–764. https://doi.org/10.1126/science.abn7760
5. Accorsi, E.K., Britton, A., Fleming-Dutra, K.E., Smith, Z.R., Shang, N., Derado, G., Miller, J., Schrag, S.J., Verani, J.R., 2022. Association Between 3 Doses of mRNA COVID-19 Vaccine and Symptomatic Infection Caused by the SARS-CoV-2 Omicron and Delta Variants. JAMA 327, 639–651. https://doi.org/10.1001/jama.2022.0470
6. Altarawneh, H.N., Chemaitelly, H., Hasan, M.R., Ayoub, H.H., Qassim, S., AlMukdad, S., Coyle, P., Yassine, H.M., Al-Khatib, H.A., Benslimane, F.M., Al-Kanaani, Z., Al-Kuwari, E., Jeremijenko, A., Kaleeckal, A.H., Latif, A.N., Shaik, R.M., Abdul-Rahim, H.F., Nasrallah, G.K., Al-Kuwari, M.G., Butt, A.A., Al-Romaihi, H.E., Al-Thani, M.H., Al-Khal, A., Bertollini, R., Tang, P., Abu-Raddad, L.J., 2022. Protection against the Omicron Variant from Previous SARS-CoV-2 Infection. New England Journal of Medicine 386, 1288–1290. https://doi.org/10.1056/NEJMc2200133
7. Cao, Y., Wang, J., Jian, F., Xiao, T., Song, W., Yisimayi, A., Huang, W., Li, Q., Wang, P., An, R., Wang, J., Wang, Yao, Niu, X., Yang, S., Liang, H., Sun, H., Li, T., Yu, Y., Cui, Q., Liu, S., Yang, X., Du, S., Zhang, Z., Hao, X., Shao, F., Jin, R., Wang, X., Xiao, J., Wang, Youchun, Xie, X.S., 2022. Omicron escapes the majority of existing SARS-CoV-2 neutralizing antibodies. Nature 602, 657–663. https://doi.org/10.1038/s41586-021-04385-3

8. Kuhlmann, C., Mayer, C.K., Claassen, M., Maponga, T., Burgers, W.A., Keeton, R., Riou, C., Sutherland, A.D., Suliman, T., Shaw, M.L., Preiser, W., 2022. Breakthrough infections with SARS-CoV-2 omicron despite mRNA vaccine booster dose. The Lancet 399, 625–626. https://doi.org/10.1016/S0140-6736(22)00090-3
9. Levin, E.G., Lustig, Y., Cohen, C., Fluss, R., Indenbaum, V., Amit, S., Doolman, R., Asraf, K., Mendelson, E., Ziv, A., Rubin, C., Freedman, L., Kreiss, Y., Regev-Yochay, G., 2021. Waning Immune Humoral Response to BNT162b2 Covid-19 Vaccine over 6 Months. New England Journal of Medicine 385, e84. https://doi.org/10.1056/NEJMoa2114583
10. Pulliam, J.R.C., van Schalkwyk, C., Govender, N., von Gottberg, A., Cohen, C., Groome, M.J., Dushoff, J., Mlisana, K., Moultrie, H., 2022. Increased risk of SARS-CoV-2 reinfection associated with emergence of Omicron in South Africa. Science 376, eabn4947. https://doi.org/10.1126/science.abn4947
11. Addetia, A., Piccoli, L., Case, J.B., Park, Y.-J., Beltramello, M., Guarino, B., Dang, H., de Melo, G.D., Pinto, D., Sprouse, K., Scheaffer, S.M., Bassi, J., Silacci-Fregni, C., Muoio, F., Dini, M., Vincenzetti, L., Acosta, R., Johnson, D., Subramanian, S., Saliba, C., Giurdanella, M., Lombardo, G., Leoni, G., Culap, K., McAlister, C., Rajesh, A., Dellota, E., Zhou, J., Farhat, N., Bohan, D., Noack, J., Chen, A., Lempp, F.A., Quispe, J., Kergoat, L., Larrous, F., Cameroni, E., Whitener, B., Giannini, O., Cippà, P., Ceschi, A., Ferrari, P., Franzetti-Pellanda, A., Biggiogero, M., Garzoni, C., Zappi, S., Bernasconi, L., Kim, M.J., Rosen, L.E., Schnell, G., Czudnochowski, N., Benigni, F., Franko, N., Logue, J.K., Yoshiyama, C., Stewart, C., Chu, H., Bourhy, H., Schmid, M.A., Purcell, L.A., Snell, G., Lanzavecchia, A., Diamond, M.S., Corti, D., Veesler, D., 2023. Neutralization, effector function and immune imprinting of Omicron variants. Nature 1–10. https://doi.org/10.1038/s41586-023-06487-6
12. Kared, H., Wolf, A.-S., Alirezaylavasani, A., Ravussin, A., Solum, G., Tran, T.T., Lund-Johansen, F., Vaage, J.T., Nissen-Meyer, L.S., Nygaard, U.C., Hungnes, O., Robertson, A.H., Næss, L.M., Trogstad, L., Magnus, P., Munthe, L.A., Mjaaland, S., 2022. Immune responses in Omicron SARS-CoV-2 breakthrough infection in vaccinated adults. Nat Commun 13, 4165. https://doi.org/10.1038/s41467-022-31888-y
13. Koutsakos, M., Lee, W.S., Reynaldi, A., Tan, H.-X., Gare, G., Kinsella, P., Liew, K.C., Taiaroa, G., Williamson, D.A., Kent, H.E., Stadler, E., Cromer, D., Khoury, D.S., Wheatley, A.K., Juno, J.A., Davenport, M.P., Kent, S.J., 2022. The magnitude and timing of recalled immunity after breakthrough infection is shaped by SARS-CoV-2 variants. Immunity 55, 1316-1326.e4. https://doi.org/10.1016/j.immuni.2022.05.018
14. Painter, M.M., Johnston, T.S., Lundgreen, K.A., Santos, J.J.S., Qin, J.S., Goel, R.R., Apostolidis, S.A., Mathew, D., Fulmer, B., Williams, J.C., McKeague, M.L., Pattekar, A., Goode, A., Nasta, S., Baxter, A.E., Giles, J.R., Skelly, A.N., Felley, L.E., McLaughlin, M., Weaver, J., Kuthuru, O., Dougherty, J., Adamski, S., Long, S., Kee, M., Clendenin, C., da Silva Antunes, R., Grifoni, A., Weiskopf, D., Sette, A., Huang, A.C., Rader, D.J., Hensley, S.E., Bates, P., Greenplate, A.R., Wherry, E.J., 2023. Prior vaccination promotes early activation of memory T cells and enhances immune responses during SARS-CoV-2 breakthrough infection. Nat Immunol 1–14. https://doi.org/10.1038/s41590-023-01613-y
15. Park, Y.-J., Pinto, D., Walls, A.C., Liu, Z., De Marco, A., Benigni, F., Zatta, F., Silacci-Fregni, C., Bassi, J., Sprouse, K.R., Addetia, A., Bowen, J.E., Stewart, C., Giurdanella, M., Saliba, C., Guarino, B., Schmid, M.A., Franko, N.M., Logue, J.K., Dang, H.V., Hauser, K., di Iulio, J., Rivera, W., Schnell, G., Rajesh, A., Zhou, J., Farhat, N., Kaiser, H., Montiel-Ruiz, M., Noack, J., Lempp, F.A., Janer, J., Abdelnabi, R., Maes, P., Ferrari, P., Ceschi, A., Giannini, O., de Melo, G.D., Kergoat, L., Bourhy, H., Neyts, J., Soriaga, L., Purcell, L.A., Snell, G., Whelan, S.P.J., Lanzavecchia, A., Virgin, H.W., Piccoli, L., Chu, H.Y., Pizzuto, M.S., Corti, D., Veesler, D., 2022. Imprinted antibody responses against

SARS-CoV-2 Omicron sublineages. Science 378, 619–627. https://doi.org/10.1126/science.adc9127

16. Wang, Z., Zhou, P., Muecksch, F., Cho, A., Ben Tanfous, T., Canis, M., Witte, L., Johnson, B., Raspe, R., Schmidt, F., Bednarski, E., Da Silva, J., Ramos, V., Zong, S., Turroja, M., Millard, K.G., Yao, K.-H., Shimeliovich, I., Dizon, J., Kaczynska, A., Jankovic, M., Gazumyan, A., Oliveira, T.Y., Caskey, M., Gaebler, C., Bieniasz, P.D., Hatziioannou, T., Nussenzweig, M.C., 2022. Memory B cell responses to Omicron subvariants after SARS-CoV-2 mRNA breakthrough infection in humans. Journal of Experimental Medicine 219, e20221006. https://doi.org/10.1084/jem.20221006
17. Weber, T., Dähling, S., Rose, S., Affeldt, P., Vanshylla, K., Ullrich, L., Gieselmann, L., Teipel, F., Gruell, H., Di Cristanziano, V., Kim, D.S., Georgiou, G., Koch, M., Kreer, C., Klein, F., 2023. Enhanced SARS-CoV-2 humoral immunity following breakthrough infection builds upon the preexisting memory B cell pool. Science Immunology 8, eadk5845. https://doi.org/10.1126/sciimmunol.adk5845
18. Yisimayi, A., Song, W., Wang, J., Jian, F., Yu, Y., Chen, X., Xu, Y., Yang, S., Niu, X., Xiao, T., Wang, J., Zhao, L., Sun, H., An, R., Zhang, N., Wang, Yao, Wang, P., Yu, L., Lv, Z., Gu, Q., Shao, F., Jin, R., Shen, Z., Xie, X.S., Wang, Youchun, Cao, Y., 2023. Repeated Omicron exposures override ancestral SARS-CoV-2 immune imprinting. Nature 1–9. https://doi.org/10.1038/s41586-023-06753-7
19. Alsoussi, W.B., Malladi, S.K., Zhou, J.Q., Liu, Z., Ying, B., Kim, W., Schmitz, A.J., Lei, T., Horvath, S.C., Sturtz, A.J., McIntire, K.M., Evavold, B., Han, F., Scheaffer, S.M., Fox, I.F., Mirza, S.F., Parra-Rodriguez, L., Nachbagauer, R., Nestorova, B., Chalkias, S., Farnsworth, C.W., Klebert, M.K., Pusic, I., Strnad, B.S., Middleton, W.D., Teefey, S.A., Whelan, S.P.J., Diamond, M.S., Paris, R., O'Halloran, J.A., Presti, R.M., Turner, J.S., Ellebedy, A.H., 2023. SARS-CoV-2 Omicron boosting induces de novo B cell response in humans. Nature 617, 592–598. https://doi.org/10.1038/s41586-023-06025-4
20. Schiepers, A., van 't Wout, M.F.L., Greaney, A.J., Zang, T., Muramatsu, H., Lin, P.J.C., Tam, Y.K., Mesin, L., Starr, T.N., Bieniasz, P.D., Pardi, N., Bloom, J.D., Victora, G.D., 2023. Molecular fate-mapping of serum antibody responses to repeat immunization. Nature 615, 482–489. https://doi.org/10.1038/s41586-023-05715-3
21. Anderson, E.M., Li, S.H., Awofolaju, M., Eilola, T., Goodwin, E., Bolton, M.J., Gouma, S., Manzoni, T.B., Hicks, P., Goel, R.R., Painter, M.M., Apostolidis, S.A., Mathew, D., Dunbar, D., Fiore, D., Brock, A., Weaver, J., Millar, J.S., DerOhannessian, S., Greenplate, A.R., Frank, I., Rader, D.J., Wherry, E.J., Bates, P., Hensley, S.E., 2022. SARS-CoV-2 infections elicit higher levels of original antigenic sin antibodies compared with SARS-CoV-2 mRNA vaccinations. Cell Reports 41, 111496. https://doi.org/10.1016/j.celrep.2022.111496
22. Arevalo, C.P., Le Sage, V., Bolton, M.J., Eilola, T., Jones, J.E., Kormuth, K.A., Nturibi, E., Balmaseda, A., Gordon, A., Lakdawala, S.S., Hensley, S.E., 2020. Original antigenic sin priming of influenza virus hemagglutinin stalk antibodies. Proceedings of the National Academy of Sciences 117, 17221–17227. https://doi.org/10.1073/pnas.1920321117
23. Coronavirus Disease 2019 [WWW Document], 2023. . Centers for Disease Control and Prevention. URL https://www.cdc.gov/media/releases/2023/p0912-COVID-19-Vaccine.html (accessed 12.21.23).
24. Selvavinayagam, S.T., Karishma, S.J., Hemashree, K., Yong, Y.K., Suvaithenamudhan, S., Rajeshkumar, M., Aswathy, B., Kalaivani, V., Priyanka, J., Kumaresan, A., Kannan, M., Gopalan, N., Chandramathi, S., Vignesh, R., Murugesan, A., Anshad, A.R., Ganesh, B., Joseph, N., Babu, H., Govindaraj, S., Larsson, M., Kandasamy, S.L., Palani, S., Singh, K., Byrareddy, S.N., Velu, V., Shankar, E.M., Raju, S., 2023. Clinical characteristics and novel mutations of omicron subvariant XBB in Tamil Nadu, India – a

cohort study. The Lancet Regional Health - Southeast Asia 19. https://doi.org/10.1016/j.lansea.2023.100272
25. Wang, Q., Iketani, S., Li, Z., Liu, Liyuan, Guo, Y., Huang, Y., Bowen, A.D., Liu, M., Wang, M., Yu, J., Valdez, R., Lauring, A.S., Sheng, Z., Wang, H.H., Gordon, A., Liu, Lihong, Ho, D.D., 2023. Alarming antibody evasion properties of rising SARS-CoV-2 BQ and XBB subvariants. Cell 186, 279-286.e8. https://doi.org/10.1016/j.cell.2022.12.018
26. TAG-VE statement on Omicron sublineages BQ.1 and XBB [WWW Document], n.d. URL https://www.who.int/news/item/27-10-2022-tag-ve-statement-on-omicron-sublineages-bq.1-and-xbb (accessed 12.21.23).
27. Auladell, M., Nguyen, T.H., Garcillán, B., Mackay, F., Kedzierska, K., Fox, A., 2019. Distinguishing naive- from memory-derived human B cells during acute responses. Clinical & Translational Immunology 8, e01090. https://doi.org/10.1002/cti2.1090
28. Chalkias, S., McGhee, N., Whatley, J.L., Essink, B., Brosz, A., Tomassini, J.E., Girard, B., Wu, K., Edwards, D.K., Nasir, A., Lee, D., Avena, L.E., Feng, J., Deng, W., Montefiori, D.C., Baden, L.R., Miller, J.M., Das, R., 2023. Safety and Immunogenicity of XBB.1.5-Containing mRNA Vaccines. https://doi.org/10.1101/2023.08.22.23293434
29. Tortorici, M.A., Addetia, A., Seo, A.J., Brown, J., Sprouse, K., Logue, J., Clarke, E., Franko, N., Chu, H., Veesler, D., 2023. Persistent immune imprinting after XBB.1.5 COVID vaccination in humans. https://doi.org/10.1101/2023.11.28.569129
30. Wang, Q., Guo, Y., Bowen, A., Mellis, I.A., Valdez, R., Gherasim, C., Gordon, A., Liu, L., Ho, D.D., 2023. XBB.1.5 monovalent mRNA vaccine booster elicits robust neutralizing antibodies against emerging SARS-CoV-2 variants. https://doi.org/10.1101/2023.11.26.568730
31. Carr, E.J., Wu, M.Y., Gahir, J., Harvey, R., Townsley, H., Bailey, C., Fowler, A.S., Dowgier, G., Hobbs, A., Herman, L., Ragno, M., Miah, M., Bawumia, P., Smith, C., Miranda, M., Mears, H.V., Adams, L., Haptipoglu, E., O'Reilly, N., Warchal, S., Sawyer, C., Ambrose, K., Kelly, G., Beale, R., Papineni, P., Corrah, T., Gilson, R., Gamblin, S., Kassiotis, G., Libri, V., Williams, B., Swanton, C., Gandhi, S., Bauer, D.L., Wall, E.C., 2023. Neutralising immunity to omicron sublineages BQ.1.1, XBB, and XBB.1.5 in healthy adults is boosted by bivalent BA.1-containing mRNA vaccination and previous Omicron infection. The Lancet Infectious Diseases 23, 781–784. https://doi.org/10.1016/S1473-3099(23)00289-X
32. Hoffmann, M., Behrens, G.M.N., Arora, P., Kempf, A., Nehlmeier, I., Cossmann, A., Manthey, L., Dopfer-Jablonka, A., Pöhlmann, S., 2023. Effect of hybrid immunity and bivalent booster vaccination on omicron sublineage neutralisation. The Lancet Infectious Diseases 23, 25–28. https://doi.org/10.1016/S1473-3099(22)00792-7
33. Lin, D.-Y., Xu, Y., Gu, Y., Zeng, D., Sunny, S.K., Moore, Z., 2023a. Durability of Bivalent Boosters against Omicron Subvariants. New England Journal of Medicine 388, 1818–1820. https://doi.org/10.1056/NEJMc2302462
34. Lin, D.-Y., Xu, Y., Gu, Y., Zeng, D., Wheeler, B., Young, H., Sunny, S.K., Moore, Z., 2023b. Effectiveness of Bivalent Boosters against Severe Omicron Infection. New England Journal of Medicine 388, 764–766. https://doi.org/10.1056/NEJMc2215471
35. Shrestha, N.K., Burke, P.C., Nowacki, A.S., Simon, J.F., Hagen, A., Gordon, S.M., 2023. Effectiveness of the Coronavirus Disease 2019 Bivalent Vaccine. Open Forum Infectious Diseases 10, ofad209. https://doi.org/10.1093/ofid/ofad209
36. Tan, Celine Y, Chiew, C.J., Pang, D., Lee, V.J., Ong, B., Lye, D.C., Tan, K.B., 2023. Protective immunity of SARS-CoV-2 infection and vaccines against medically attended symptomatic omicron BA.4, BA.5, and XBB reinfections in Singapore: a national cohort study. The Lancet Infectious Diseases 23, 799–805. https://doi.org/10.1016/S1473-3099(23)00060-9

37. Tan, Celine Y., Chiew, C.J., Pang, D., Lee, V.J., Ong, B., Wang, L.-F., Ren, E.C., Lye, D.C., Tan, K.B., 2023. Effectiveness of bivalent mRNA vaccines against medically attended symptomatic SARS-CoV-2 infection and COVID-19-related hospital admission among SARS-CoV-2-naive and previously infected individuals: a retrospective cohort study. The Lancet Infectious Diseases 0. https://doi.org/10.1016/S1473-3099(23)00373-0
38. Werkhoven, C.H. van, Valk, A.-W., Smagge, B., Melker, H.E. de, Knol, M.J., Hahné, S.J.M., Hof, S. van den, Gier, B. de, 2023. Early COVID-19 vaccine effectiveness of XBB.1.5 vaccine against hospitalization and ICU admission, the Netherlands, 9 October - 5 December 2023. https://doi.org/10.1101/2023.12.12.23299855
39. Wang, Q., Bowen, A., Tam, A.R., Valdez, R., Stoneman, E., Mellis, I.A., Gordon, A., Liu, L., Ho, D.D., 2023a. SARS-CoV-2 neutralising antibodies after bivalent versus monovalent booster. The Lancet Infectious Diseases 23, 527–528. https://doi.org/10.1016/S1473-3099(23)00181-0
40. Bergström, J.J.E., Xu, H., Heyman, B., 2017. Epitope-Specific Suppression of IgG Responses by Passively Administered Specific IgG: Evidence of Epitope Masking. Front Immunol 8, 238. https://doi.org/10.3389/fimmu.2017.00238
41. Schaefer-Babajew, D., Wang, Z., Muecksch, F., Cho, A., Loewe, M., Cipolla, M., Raspe, R., Johnson, B., Canis, M., DaSilva, J., Ramos, V., Turroja, M., Millard, K.G., Schmidt, F., Witte, L., Dizon, J., Shimeliovich, I., Yao, K.-H., Oliveira, T.Y., Gazumyan, A., Gaebler, C., Bieniasz, P.D., Hatziioannou, T., Caskey, M., Nussenzweig, M.C., 2023. Antibody feedback regulates immune memory after SARS-CoV-2 mRNA vaccination. Nature 613, 735–742. https://doi.org/10.1038/s41586-022-05609-w
42. Tas, J.M.J., Koo, J.-H., Lin, Y.-C., Xie, Z., Steichen, J.M., Jackson, A.M., Hauser, B.M., Wang, X., Cottrell, C.A., Torres, J.L., Warner, J.E., Kirsch, K.H., Weldon, S.R., Groschel, B., Nogal, B., Ozorowski, G., Bangaru, S., Phelps, N., Adachi, Y., Eskandarzadeh, S., Kubitz, M., Burton, D.R., Lingwood, D., Schmidt, A.G., Nair, U., Ward, A.B., Schief, W.R., Batista, F.D., 2022. Antibodies from primary humoral responses modulate the recruitment of naive B cells during secondary responses. Immunity 55, 1856-1871.e6. https://doi.org/10.1016/j.immuni.2022.07.020
43. Lim, W.W., Mak, L., Leung, G.M., Cowling, B.J., Peiris, M., 2021. Comparative immunogenicity of mRNA and inactivated vaccines against COVID-19. The Lancet Microbe 2, e423. https://doi.org/10.1016/S2666-5247(21)00177-4
44. Premikha, M., Chiew, C.J., Wei, W.E., Leo, Y.S., Ong, B., Lye, D.C., Lee, V.J., Tan, K.B., 2022. Comparative Effectiveness of mRNA and Inactivated Whole-Virus Vaccines Against Coronavirus Disease 2019 Infection and Severe Disease in Singapore. Clinical Infectious Diseases 75, 1442–1445. https://doi.org/10.1093/cid/ciac288
45. Arevalo, P., McLean, H.Q., Belongia, E.A., Cobey, S., 2020. Earliest infections predict the age distribution of seasonal influenza A cases. eLife 9, e50060. https://doi.org/10.7554/eLife.50060
46. Gostic, K.M., Bridge, R., Brady, S., Viboud, C., Worobey, M., Lloyd-Smith, J.O., 2019. Childhood immune imprinting to influenza A shapes birth year-specific risk during seasonal H1N1 and H3N2 epidemics. PLOS Pathogens 15, e1008109. https://doi.org/10.1371/journal.ppat.1008109
47. Gostic, K.M., Ambrose, M., Worobey, M., Lloyd-Smith, J.O., 2016. Potent protection against H5N1 and H7N9 influenza via childhood hemagglutinin imprinting. Science 354, 722–726. https://doi.org/10.1126/science.aag1322

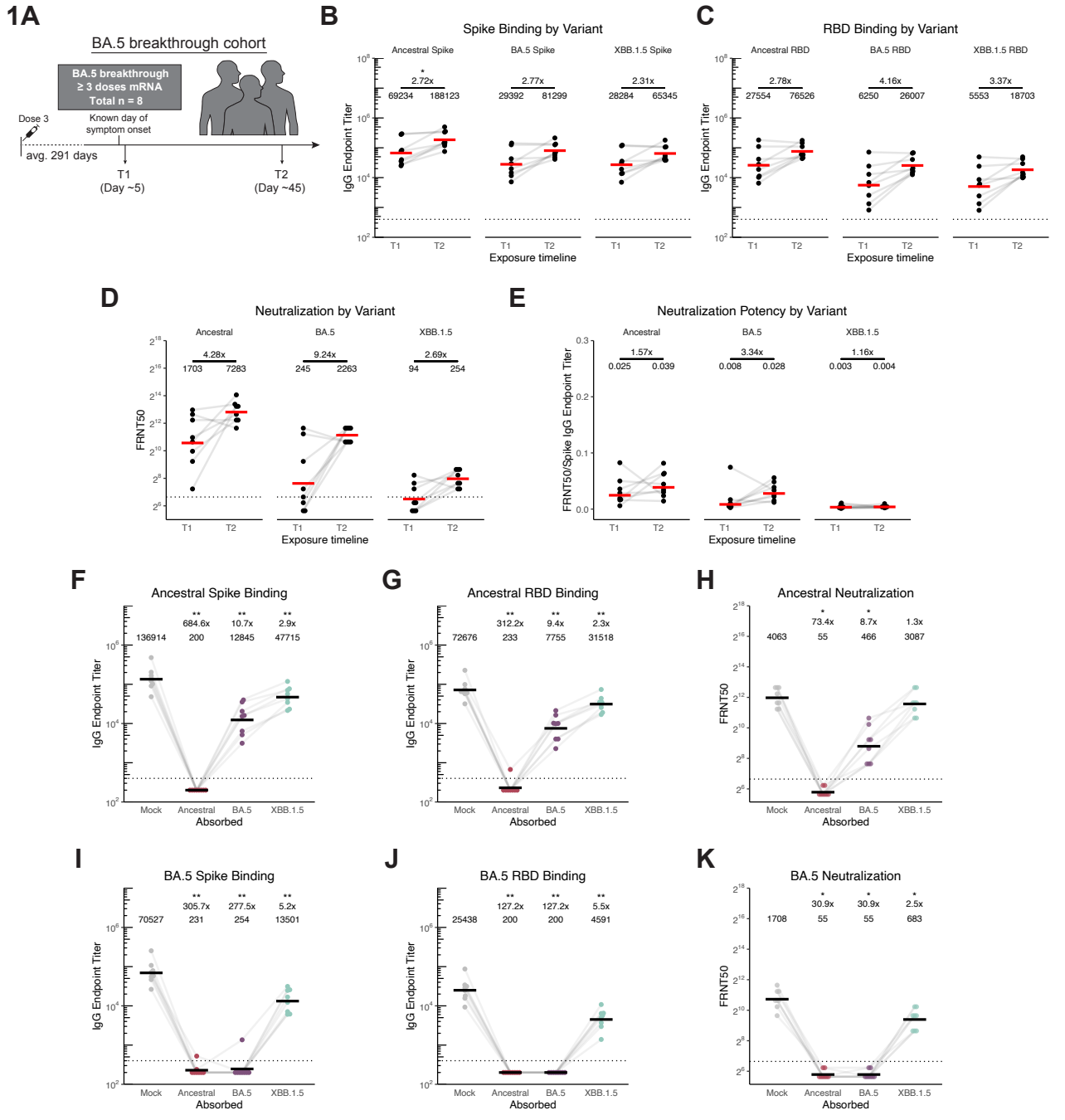
1A
BA.5 breakthrough cohort
BA.5 breakthrough
≥ 3 doses mRNA
Total n = 8
Dose 3
Known day of
symptom onset
avg. 291 days
T1
(Day ~5)
T2
(Day ~45)
B
Spike Binding by Variant
Ancestral Spike
BA.5 Spike
XBB.1.5 Spike
IgG Endpoint Titer
2.72x
69234
188123
2.77x
29392
81299
2.31x
28284
65345
T1
T2
Exposure timeline
C
RBD Binding by Variant
Ancestral RBD
BA.5 RBD
XBB.1.5 RBD
2.78x
27554
76526
4.16x
6250
26007
3.37x
5553
18703
D
Neutralization by Variant
Ancestral
BA.5
XBB.1.5
FRNT50
4.28x
1703
7283
9.24x
245
2263
2.69x
94
254
E
Neutralization Potency by Variant
FRNT50/Spike IgG Endpoint Titer
1.57x
0.025
0.039
3.34x
0.008
0.028
1.16x
0.003
0.004
F
Ancestral Spike Binding
684.6x
136914
200
10.7x
12845
2.9x
47715
Mock
Ancestral
BA.5
XBB.1.5
Absorbed
G
Ancestral RBD Binding
312.2x
72676
233
9.4x
7755
2.3x
31518
H
Ancestral Neutralization
73.4x
4063
55
8.7x
466
1.3x
3087
I
BA.5 Spike Binding
305.7x
70527
231
277.5x
254
5.2x
13501
J
BA.5 RBD Binding
127.2x
25438
200
127.2x
200
5.5x
4591
K
BA.5 Neutralization
30.9x
1708
55
30.9x
55
2.5x
683

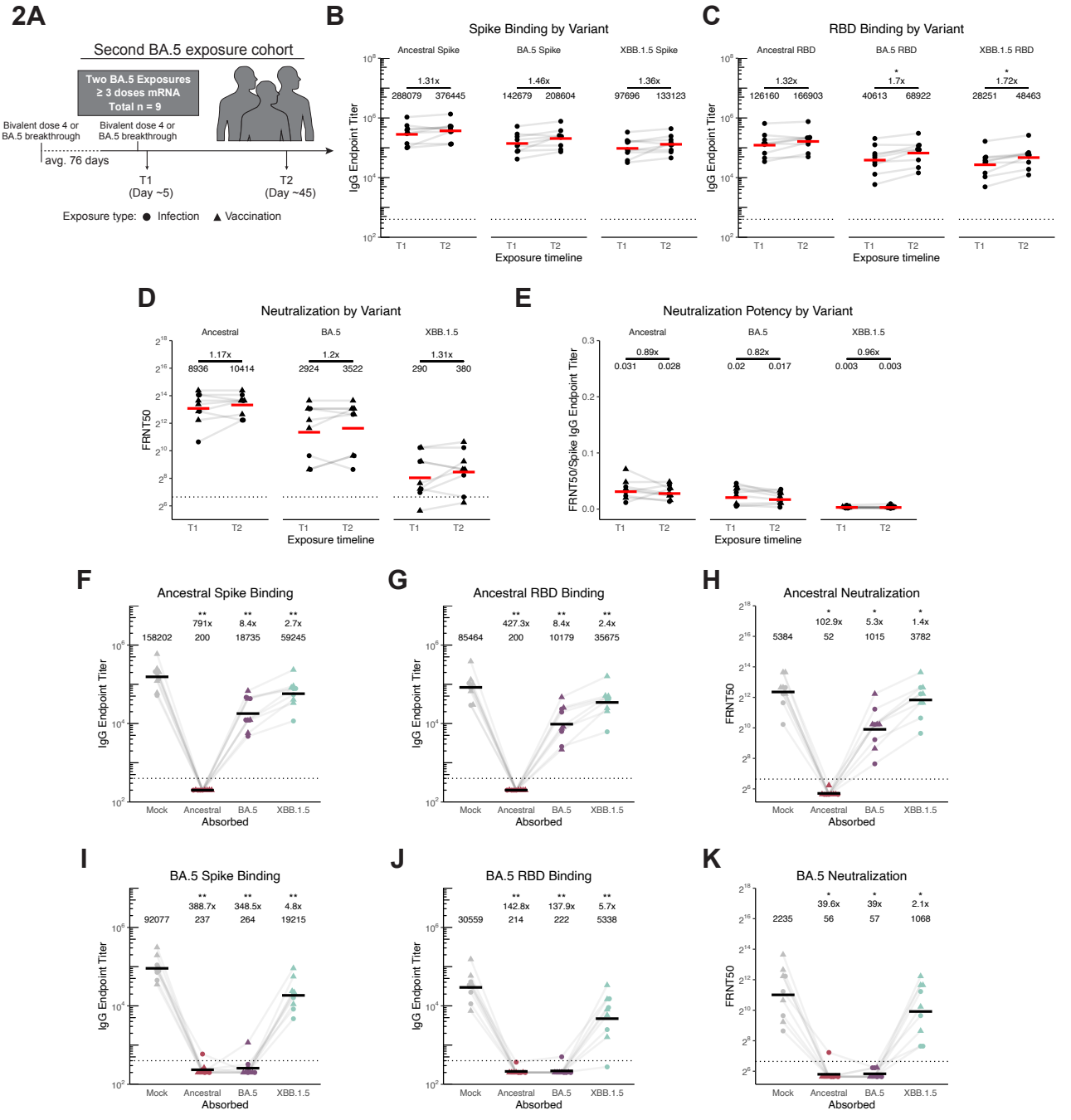
2A
Second BA.5 exposure cohort
Two BA.5 Exposures
≥ 3 doses mRNA
Total n = 9
Bivalent dose 4 or BA.5 breakthrough
Bivalent dose 4 or BA.5 breakthrough
avg. 76 days
T1 (Day ~5)
T2 (Day ~45)
Exposure type: ● Infection ▲ Vaccination
B
Spike Binding by Variant
Ancestral Spike
BA.5 Spike
XBB.1.5 Spike
IgG Endpoint Titer
1.31x
288079 376445
1.46x
142679 208604
1.36x
97696 133123
T1 T2
Exposure timeline
C
RBD Binding by Variant
Ancestral RBD
BA.5 RBD
XBB.1.5 RBD
1.32x
126160 166903
1.7x
40613 68922
1.72x
28251 48463
D
Neutralization by Variant
Ancestral
BA.5
XBB.1.5
FRNT50
1.17x
8936 10414
1.2x
2924 3522
1.31x
290 380
E
Neutralization Potency by Variant
FRNT50/Spike IgG Endpoint Titer
0.89x
0.031 0.028
0.82x
0.02 0.017
0.96x
0.003 0.003
F
Ancestral Spike Binding
158202
791x 200
8.4x 18735
2.7x 59245
Mock Ancestral BA.5 XBB.1.5
Absorbed
G
Ancestral RBD Binding
85464
427.3x 200
8.4x 10179
2.4x 35675
H
Ancestral Neutralization
5384
102.9x 52
5.3x 1015
1.4x 3782
I
BA.5 Spike Binding
92077
388.7x 237
348.5x 264
4.8x 19215
J
BA.5 RBD Binding
30559
142.8x 214
137.9x 222
5.7x 5338
K
BA.5 Neutralization
2235
39.6x 56
39x 57
2.1x 1068

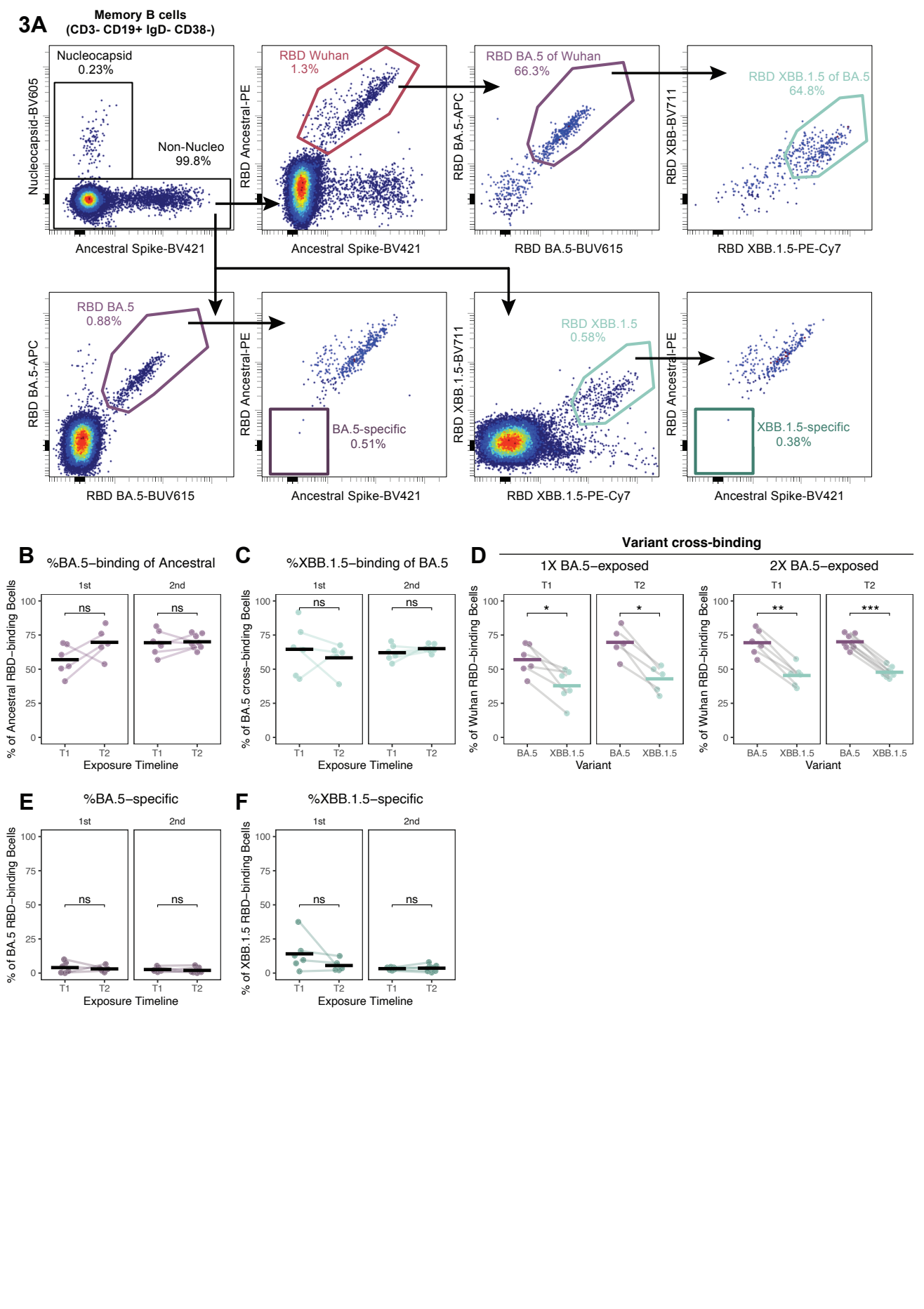
3A
Memory B cells
(CD3- CD19+ IgD- CD38-)
Nucleocapsid
0.23%
Non-Nucleo
99.8%
Nucleocapsid-BV605
Ancestral Spike-BV421
RBD Wuhan
1.3%
RBD Ancestral-PE
Ancestral Spike-BV421
RBD BA.5 of Wuhan
66.3%
RBD BA.5-APC
RBD BA.5-BUV615
RBD XBB.1.5 of BA.5
64.8%
RBD XBB-BV711
RBD XBB.1.5-PE-Cy7
RBD BA.5
0.88%
RBD BA.5-APC
RBD BA.5-BUV615
BA.5-specific
0.51%
RBD Ancestral-PE
Ancestral Spike-BV421
RBD XBB.1.5
0.58%
RBD XBB.1.5-BV711
RBD XBB.1.5-PE-Cy7
XBB.1.5-specific
0.38%
RBD Ancestral-PE
Ancestral Spike-BV421
B
%BA.5–binding of Ancestral
1st
2nd
ns
% of Ancestral RBD–binding Bcells
T1
T2
Exposure Timeline
C
%XBB.1.5–binding of BA.5
% of BA.5 cross–binding Bcells
D
Variant cross-binding
1X BA.5–exposed
2X BA.5–exposed
T1
T2
*
**
***
% of Wuhan RBD–binding Bcells
BA.5
XBB.1.5
Variant
E
%BA.5–specific
% of BA.5 RBD–binding Bcells
F
%XBB.1.5–specific
% of XBB.1.5 RBD–binding Bcells

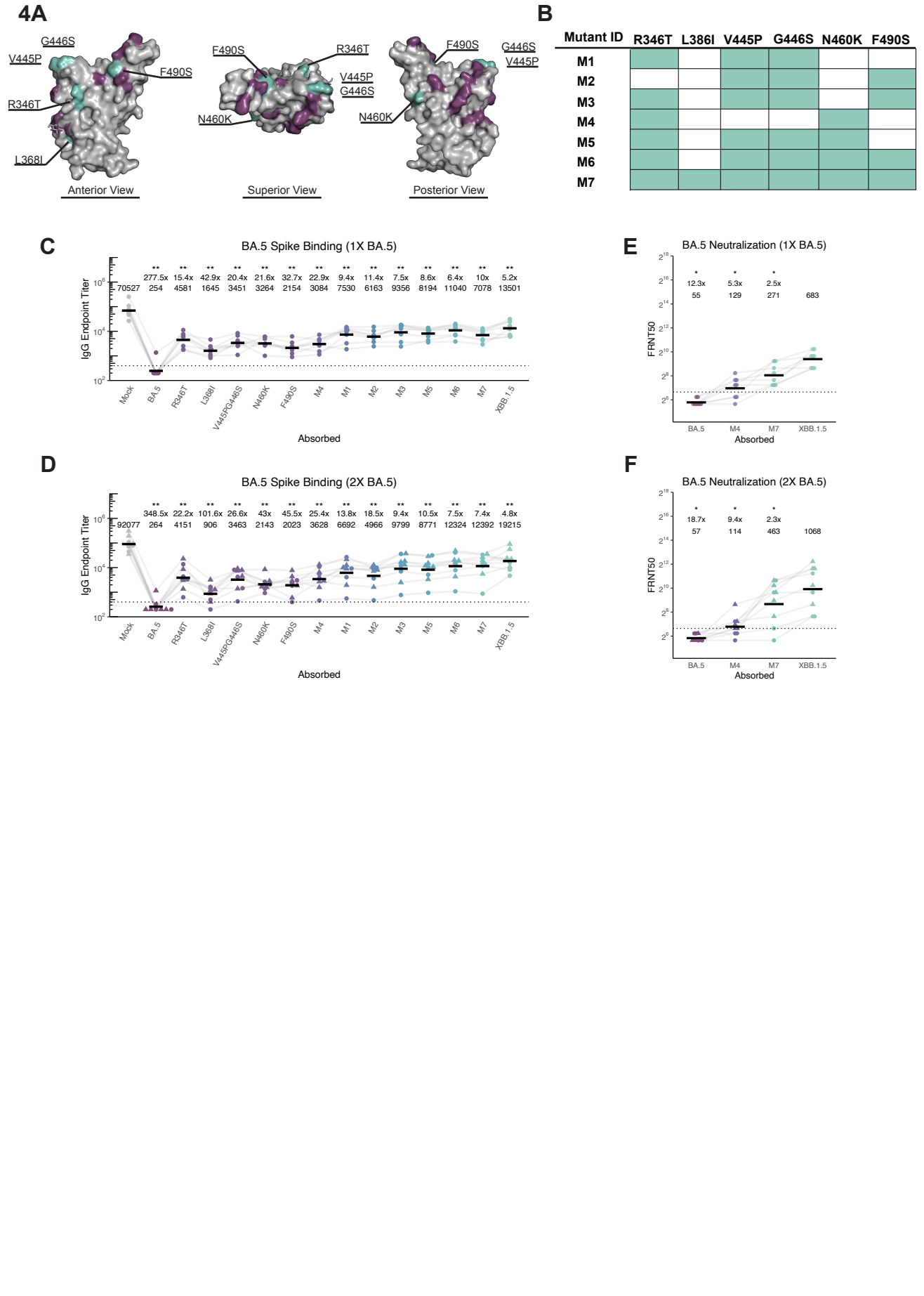
4A
G446S
V445P
F490S
R346T
L368I
Anterior View
F490S
R346T
V445P
G446S
N460K
Superior View
F490S
G446S
V445P
N460K
Posterior View
B
Mutant ID
R346T
L386I
V445P
G446S
N460K
F490S
M1
M2
M3
M4
M5
M6
M7
C
BA.5 Spike Binding (1X BA.5)
IgG Endpoint Titer
70527
277.5x 15.4x 42.9x 20.4x 21.6x 32.7x 22.9x 9.4x 11.4x 7.5x 8.6x 6.4x 10x 5.2x
254 4581 1645 3451 3264 2154 3084 7530 6163 9356 8194 11040 7078 13501
Mock BA.5 R346T L368I V445P/G446S N460K F490S M4 M1 M2 M3 M5 M6 M7 XBB.1.5
Absorbed
D
BA.5 Spike Binding (2X BA.5)
IgG Endpoint Titer
92077
348.5x 22.2x 101.6x 26.6x 43x 45.5x 25.4x 13.8x 18.5x 9.4x 10.5x 7.5x 7.4x 4.8x
264 4151 906 3463 2143 2023 3628 6692 4966 9799 8771 12324 12392 19215
Mock BA.5 R346T L368I V445P/G446S N460K F490S M4 M1 M2 M3 M5 M6 M7 XBB.1.5
Absorbed
E
BA.5 Neutralization (1X BA.5)
FRNT50
12.3x 5.3x 2.5x
55 129 271 683
BA.5 M4 M7 XBB.1.5
Absorbed
F
BA.5 Neutralization (2X BA.5)
FRNT50
18.7x 9.4x 2.3x
57 114 463 1068
BA.5 M4 M7 XBB.1.5
Absorbed

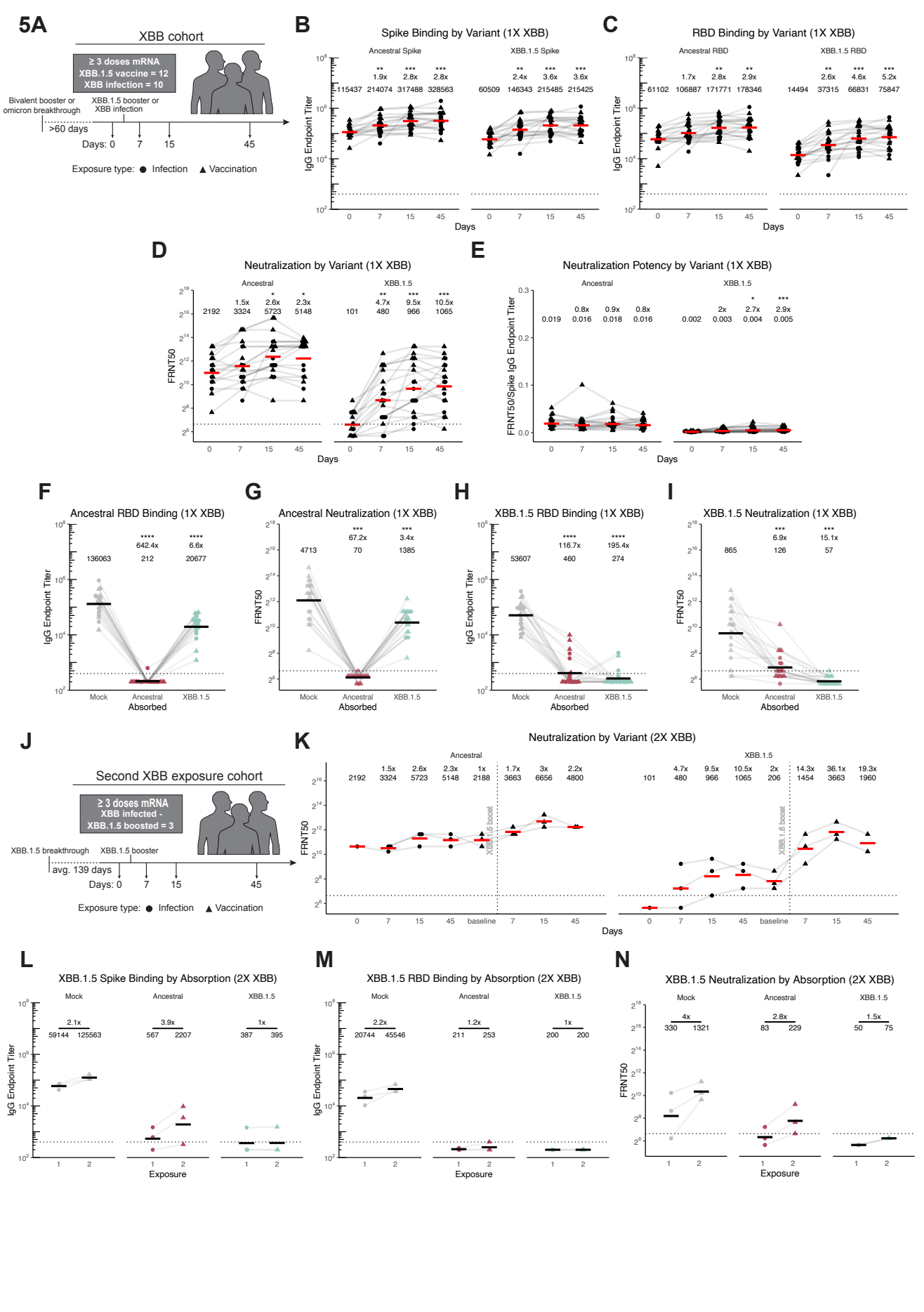
5A
XBB cohort
≥ 3 doses mRNA
XBB.1.5 vaccine = 12
XBB infection = 10
Bivalent booster or
omicron breakthrough
XBB.1.5 booster or
XBB infection
>60 days
Days: 0
7
15
45
Exposure type: ● Infection ▲ Vaccination
B
Spike Binding by Variant (1X XBB)
Ancestral Spike
XBB.1.5 Spike
IgG Endpoint Titer
Days
C
RBD Binding by Variant (1X XBB)
Ancestral RBD
XBB.1.5 RBD
IgG Endpoint Titer
Days
D
Neutralization by Variant (1X XBB)
Ancestral
XBB.1.5
FRNT50
Days
E
Neutralization Potency by Variant (1X XBB)
Ancestral
XBB.1.5
FRNT50/Spike IgG Endpoint Titer
Days
F
Ancestral RBD Binding (1X XBB)
IgG Endpoint Titer
Mock
Ancestral
XBB.1.5
Absorbed
G
Ancestral Neutralization (1X XBB)
FRNT50
Mock
Ancestral
XBB.1.5
Absorbed
H
XBB.1.5 RBD Binding (1X XBB)
IgG Endpoint Titer
Mock
Ancestral
XBB.1.5
Absorbed
I
XBB.1.5 Neutralization (1X XBB)
FRNT50
Mock
Ancestral
XBB.1.5
Absorbed
J
Second XBB exposure cohort
≥ 3 doses mRNA
XBB infected -
XBB.1.5 boosted = 3
XBB.1.5 breakthrough
XBB.1.5 booster
avg. 139 days
Days: 0
7
15
45
Exposure type: ● Infection ▲ Vaccination
K
Neutralization by Variant (2X XBB)
Ancestral
XBB.1.5
FRNT50
XBB.1.5 boost
baseline
Days
L
XBB.1.5 Spike Binding by Absorption (2X XBB)
Mock
Ancestral
XBB.1.5
IgG Endpoint Titer
Exposure
M
XBB.1.5 RBD Binding by Absorption (2X XBB)
Mock
Ancestral
XBB.1.5
IgG Endpoint Titer
Exposure
N
XBB.1.5 Neutralization by Absorption (2X XBB)
Mock
Ancestral
XBB.1.5
FRNT50
Exposure

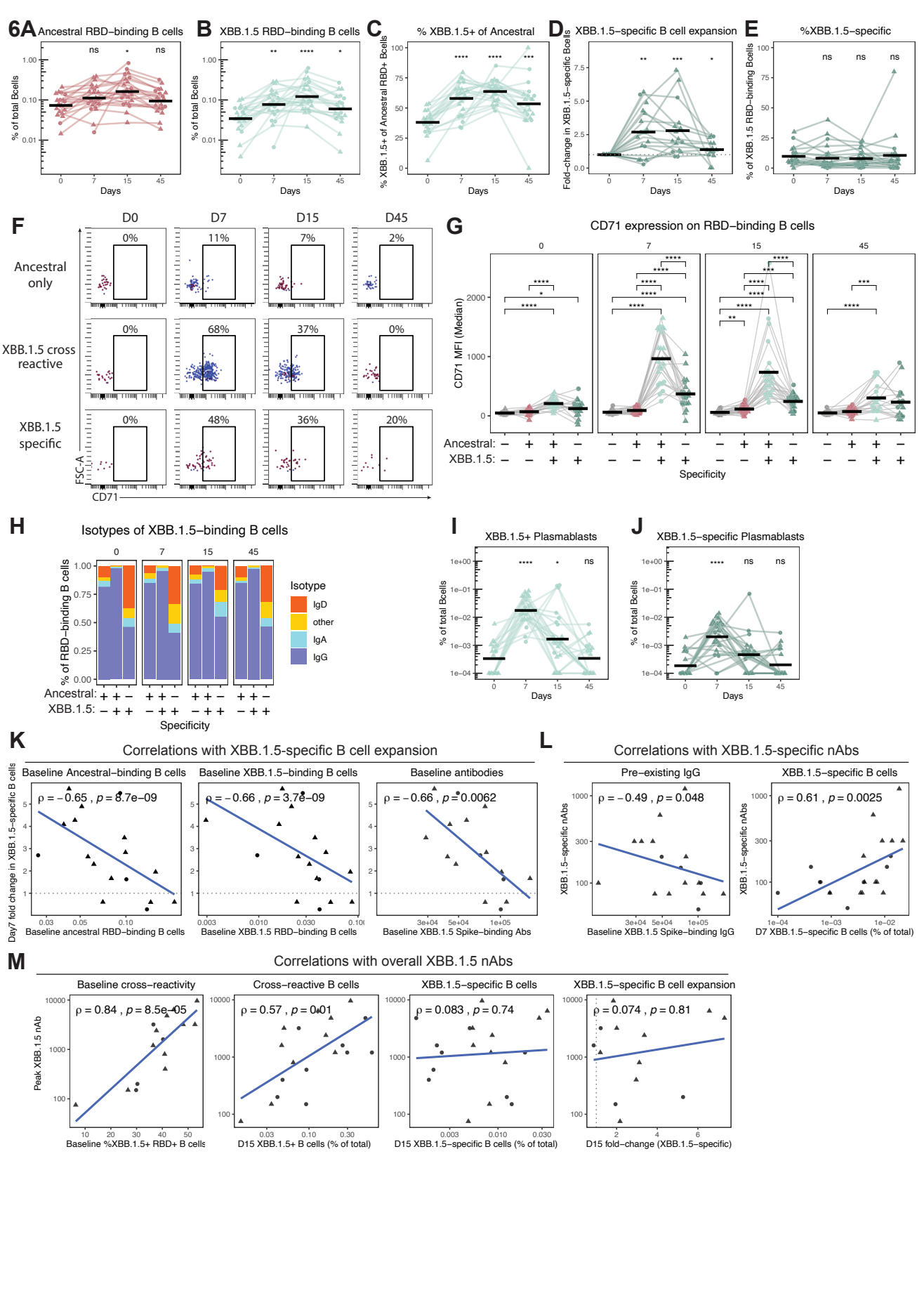
6A
Ancestral RBD−binding B cells
% of total Bcells
Days
B
XBB.1.5 RBD−binding B cells
C
% XBB.1.5+ of Ancestral
% XBB.1.5+ of Ancestral RBD+ Bcells
D
XBB.1.5−specific B cell expansion
Fold−change in XBB.1.5−specific Bcells
E
%XBB.1.5−specific
% of XBB.1.5 RBD−binding Bcells
F
D0
D7
D15
D45
Ancestral only
XBB.1.5 cross reactive
XBB.1.5 specific
0%
11%
7%
2%
0%
68%
37%
0%
0%
48%
36%
20%
FSC−A
CD71
G
CD71 expression on RBD−binding B cells
CD71 MFI (Median)
Ancestral:
XBB.1.5:
Specificity
H
Isotypes of XBB.1.5−binding B cells
% of RBD−binding B cells
Isotype
IgD
other
IgA
IgG
I
XBB.1.5+ Plasmablasts
J
XBB.1.5−specific Plasmablasts
K
Correlations with XBB.1.5−specific B cell expansion
Baseline Ancestral−binding B cells
ρ = −0.65 , p = 8.7e−09
Baseline XBB.1.5−binding B cells
ρ = −0.66 , p = 3.7e−09
Baseline antibodies
ρ = −0.66 , p = 0.0062
Day7 fold change in XBB.1.5−specific B cells
Baseline ancestral RBD−binding B cells
Baseline XBB.1.5 RBD−binding B cells
Baseline XBB.1.5 Spike−binding Abs
L
Correlations with XBB.1.5−specific nAbs
Pre−existing IgG
ρ = −0.49 , p = 0.048
XBB.1.5−specific B cells
ρ = 0.61 , p = 0.0025
XBB.1.5−specific nAbs
Baseline XBB.1.5 Spike−binding IgG
D7 XBB.1.5−specific B cells (% of total)
M
Correlations with overall XBB.1.5 nAbs
Baseline cross−reactivity
ρ = 0.84 , p = 8.5e−05
Cross−reactive B cells
ρ = 0.57 , p = 0.01
XBB.1.5−specific B cells
ρ = 0.083 , p = 0.74
XBB.1.5−specific B cell expansion
ρ = 0.074 , p = 0.81
Peak XBB.1.5 nAb
Baseline %XBB.1.5+ RBD+ B cells
D15 XBB.1.5+ B cells (% of total)
D15 XBB.1.5−specific B cells (% of total)
D15 fold−change (XBB.1.5−specific)